KSCE Journal of Civil Engineering (2018) 22(4):1235-1249

DOI 10.1007/s12205-017-1517-6

Structural Engineering

pISSN 1226-7988, eISSN 1976-3808
www.springer.com/12205

A Simplified First-order Shear Deformation Theory for Bending, Buckling and Free Vibration Analyses of Isotropic Plates on Elastic Foundations

Minwo Park* and Dong-Ho Choi**

Received February 3, 2016/Accepted April 5, 2017/Published Online June 30, 2017

Abstract

This paper presents analytical solutions for bending, buckling and free vibration analyses of isotropic plates on elastic foundations using a simplified first-order shear deformation theory. Unlike the conventional first-order shear deformation theory, the present theory contains only two variables and has many similarities to the classical plate theory. For the elastic foundations, the Pasternak model which has two parameters is used. Equations of motion are derived from Hamilton's principle. Analytical solutions of deflections, moments, shear forces, buckling loads and natural frequencies are obtained for rectangular plates with various boundary conditions. Numerical examples for various aspect ratios, side-to-thickness ratios and foundation parameters are presented to verify the validity of the present theory. Comparative study shows that the present theory is accurate and efficient in predicting bending, buckling and free vibration responses of isotropic plates on elastic foundations. Parametric study shows the effect of the elastic foundations on the behavior of the plates.

Keywords: *plates, bending, buckling, vibration, elastic foundations, first-order shear deformation theory*

1. Introduction

Bending, buckling and free vibration responses of isotropic plates on elastic foundations have been studied by many researchers. To describe the interaction between the plate and the foundations, various kinds of foundation models have been proposed. The simplest is that proposed by Winkler (1867), in which the foundation is modeled as a series of separated springs without coupling effects between each other. Pasternak (1954) improved this model by adding a shear spring to simulate interaction among the separated springs in the Winkler model. The Pasternak (two-parameter) model has been used to describe the interaction between the structure and the foundation, and this is used herein to model the interaction between the plate and the foundation.

The bending, buckling and free vibration responses of the isotropic plates on the elastic foundations can be predicted by two-dimensional plate theories such as the classical plate theory (CPT) (Leissa, 1973; Yettram *et al.*, 1984; Lam *et al.*, 2000; Huang and Thambiratnam, 2001; Chucheepsakul and Chinnaboon, 2002; Civalek, 2007a), the first-order shear deformation theory (FSDT) (Yen and Tang, 1971; Henwood *et al.*, 1982; Kobayashi and Sonoda, 1989; Xiang *et al.*, 1994; Qin, 1995; Liew *et al.*, 1996; Eratll and Akoz, 1997; Han and Liew, 1997; Shen, 1999; Liu, 2000; Shen, 2000; Buczkowski and Torbacki, 2001; Shen *et al.*, 2001; Xiang, 2003; Abdalla and Ibrahim, 2006; Ozgan and Daloglu, 2007; Akhavan *et al.*, 2009a; 2009b; Ferreira *et al.,* 2010; Ferreira et al, 2011; Nobakhti and Aghdam, 2011; Zenkour *et al.*, 2011), higher-order shear deformation theories (HSDTs) (Wang *et al.*, 1997; Matsunaga, 2000; Zenkour, 2009; Thai and Choi, 2011; 2012; Thai *et al.*, 2013), and three-dimensional elasticity theories (Zhou *et al.*, 2004; Civalek, 2007b; Dehghan and Baradaran, 2011). The CPT provides good predictions for thin plates only. For thick plates, it underestimates deflections and overestimates buckling loads and natural frequencies due to ignoring shear deformation effects. The FSDT considers the shear deformation effect by way of linear variations of in-plane displacements through the thickness, but it requires a shear correction factor to satisfy the free transverse shear stress conditions on the top and bottom surfaces of the plate. A large number of researchers have employed the FSDT to predict the bending, buckling and free vibration responses of the thick plates, but it is difficult to determine the correct value of the shear correction factor. To avoid the use of the shear correction factor and obtain a better prediction of responses of thick plates, HSDTs have been developed, and although they offer a slight improvement in accuracy compared to the FSDT, their equations of motion are much more complicated. Therefore, it is necessary to develop a theory which is not only accurate but also simple to use.

Endo and Kimura (2007) and Endo (2015) proposed a simplified

*Ph.D. Candidate, Dept. of Civil and Environmental Engineering, Hanyang University, Seoul 04763, Korea (E-mail: mwpark00@gmail.com)
**Member, Professor, Dept. of Civil and Environmental Engineering, Hanyang University, Seoul 04763, Korea (Corresponding Author, E-mail: samga@hanyang.ac.kr)

FSDT separating the transverse displacement into bending and shear parts, and demonstrated its accuracy for free vibration analysis of isotropic beams and plates. Unlike the conventional FSDT, this simplified FSDT involves only two variables and two governing equations while the conventional one has three of each. Moreover, it has strong similarities to the CPT in many aspects such as the equations of motion, boundary conditions and stress resultants. The simplified FSDT was extended to simply supported orthotropic plates by Shimpi *et al.* (2007) for the bending and free vibration analyses. Thai and Choi (2013a, 2013b) extended it to simply supported laminated composite plates (Thai and Choi, 2013a) and functionally graded plates (Thai and Choi, 2013b) for these analyses. Recently, Yin *et al.* (2014) extended the simplified FSDT to functionally graded plates with various boundary conditions for bending and free vibration analyses using an Isogeometric Analysis (IGA). So far, however, the buckling analysis has not been carried out, nor has it been applied to the plates on elastic foundations.

In this paper, the simplified FSDT was extended to bending, buckling and free vibration analyses of isotropic plates on elastic foundations using the Pasternak model. The equations of motion are derived from Hamilton's principle. Analytical solutions of deflections, buckling loads and natural frequencies are obtained for rectangular plates with various boundary conditions. Numerical examples for various aspect ratios, side-to-thickness ratios and foundation parameters are presented to verify the validity of the present theory.

2. Equations of Motion

2.1 Constitutive Equations

For isotropic plates, the constitutive equations for the stress-strain relations can be expressed in a matrix form as

$$\begin{Bmatrix} \sigma_x \\ \sigma_y \\ \tau_{xy} \\ \tau_{yz} \\ \tau_{xz} \end{Bmatrix} = \frac{E}{1-\nu^2} \begin{bmatrix} 1 & \nu & 0 & 0 & 0 \\ \nu & 1 & 0 & 0 & 0 \\ 0 & 0 & \frac{1-\nu}{2} & 0 & 0 \\ 0 & 0 & 0 & \frac{1-\nu}{2} & 0 \\ 0 & 0 & 0 & 0 & \frac{1-\nu}{2} \end{bmatrix} \begin{Bmatrix} \varepsilon_x \\ \varepsilon_y \\ \gamma_{xy} \\ \gamma_{yz} \\ \gamma_{xz} \end{Bmatrix} \tag{1}$$

where E is Young's modulus, and ν is Poisson's ratio for the plate.

The moments (M_x, M_y, M_{xy}) and the transverse shear forces (Q_x, Q_y) are given by

$$(M_x, M_y, M_{xy}) = \int_{-h/2}^{h/2} (\sigma_x, \sigma_y, \sigma_{xy}) z dz \tag{2a}$$

$$(Q_x, Q_y) = \int_{-h/2}^{h/2} (\sigma_{xz}, \sigma_{yz}) dz \tag{2b}$$

2.2. Displacements and Strains

The displacement field of the simplified FSDT is derived by applying further assumptions (Buczkowski and Torbacki, 2001; Shen *et al.*, 2001; Xiang, 2003; Abdalla and Ibrahim, 2006; Ozgan and Daloglu, 2007) to the conventional FSDT. The displacement field of the conventional FSDT is given by

$$\begin{aligned} u_x(x, y, z, t) &= z\theta_x(x, y, t) \\ u_y(x, y, z, t) &= z\theta_y(x, y, t) \\ u_z(x, y, z, t) &= w(x, y, t) \end{aligned} \tag{3}$$

where w, θ_x and θ_y are three unknown functions of the midplane of the plate. By separating the transverse displacement w into a bending part w_b and a shear part w_s and assuming that the rotations are $\theta_x = -\partial w_b/\partial w_b$ and $\theta_y = -\partial w_b/\partial y$, the displacement field can be rewritten as

$$\begin{aligned} u_x(x, y, z, t) &= -z\frac{\partial w_b(x, y, t)}{\partial x} \\ u_y(x, y, z, t) &= -z\frac{\partial w_b(x, y, t)}{\partial y} \\ u_z(x, y, z, t) &= w_b(x, y, t) + w_s(x, y, t) \end{aligned} \tag{4}$$

From the displacement field in Eqs. (4), the linear strains are written as

$$\begin{aligned} \varepsilon_x &= \frac{\partial u_x}{\partial x} = -z\frac{\partial^2 w_b}{\partial x^2} & \gamma_{xy} &= \frac{\partial u_x}{\partial y} + \frac{\partial u_y}{\partial x} = -2z\frac{\partial^2 w_b}{\partial x \partial y} \\ \varepsilon_y &= \frac{\partial u_y}{\partial y} = -z\frac{\partial^2 w_b}{\partial y^2} & \gamma_{yz} &= \frac{\partial u_y}{\partial z} + \frac{\partial u_z}{\partial y} = \frac{\partial w_s}{\partial y} \\ \varepsilon_z &= \frac{\partial u_z}{\partial z} = 0 & \gamma_{xz} &= \frac{\partial u_x}{\partial z} + \frac{\partial u_z}{\partial x} = \frac{\partial w_s}{\partial x} \end{aligned} \tag{5}$$

2.3 Equations of Motion

Hamilton's principle is used to derive the equations of motion. It can be expressed in an analytical form as (Reddy, 2002)

$$0 = \int_0^T (\delta U_P + \delta U_F + \delta V - \delta K) dt \tag{6}$$

where δU_P and δU_F are the virtual strain energy of the plate and the foundations, respectively; δV is the virtual work done by applied forces; and δK is the virtual kinetic energy. The virtual strain energy of the plate is obtained by using Eqs. (1) and (2):

$$\begin{aligned} \delta U_P &= \int_A \int_{-h/2}^{h/2} (\sigma_x \delta\varepsilon_x + \sigma_y \delta\varepsilon_y + \tau_{xy}\delta\gamma_{xy} + \tau_{xz}\delta\gamma_{xz} + \tau_{yz}\delta\gamma_{yz}) dz dA \\ &= \int_A \left(-M_x \frac{\partial^2 \delta w_b}{\partial x^2} - M_y \frac{\partial^2 \delta w_b}{\partial y^2} - 2M_{xy}\frac{\partial^2 \delta w_b}{\partial x \partial y} + Q_x \frac{\partial \delta w_s}{\partial x} + Q_y \frac{\partial \delta w_s}{\partial y} \right) dA \end{aligned} \tag{7}$$

The virtual strain energy of the foundations is given by

$$\delta U_F = \int_A \left[K_w u_z \delta w + K_s \left(\frac{\partial u_z}{\partial x}\frac{\partial \delta u_z}{\partial x} + \frac{\partial u_z}{\partial y}\frac{\partial \delta u_z}{\partial y} \right) \right] dA \tag{8}$$

where K_w and K_s are transverse and shear stiffness coefficients of the foundations, respectively. The virtual work done by applied forces is given by

$$\begin{aligned} \delta V = -\int_A q\,\delta u_z dA + \int_A \bigg[& N_x^0 \frac{\partial u_z}{\partial x}\frac{\partial \delta u_z}{\partial x} + N_{xy}^0 \left(\frac{\partial \delta u_z}{\partial x}\frac{\partial u_z}{\partial y} + \frac{\partial u_z}{\partial x}\frac{\partial \delta u_z}{\partial y} \right) \\ & + N_y^0 \frac{\partial u}{\partial y}\frac{\partial \delta u_z}{\partial y} \bigg] dA \end{aligned} \tag{9}$$

where q and (N_x^0, N_y^0, N_{xy}^0) are transverse and in-plane applied loads, respectively. The virtual kinetic energy is given by

$$\delta K = \int_A \int_{-h/2}^{h/2} \rho\left(\dot{u}_x \delta \dot{u}_x + \dot{u}_y \delta \dot{u}_y + \dot{u}_z \delta \dot{u}_z\right) dz dA$$
$$= \int_A \left[I_0 \left(\dot{w}_b + \dot{w}_s\right) \delta\left(\dot{w}_b + \dot{w}_s\right) + I_2 \left(\frac{\partial \dot{w}_b}{\partial x} \frac{\partial \delta \dot{w}_b}{\partial x} + \frac{\partial \dot{w}_b}{\partial y} \frac{\partial \delta \dot{w}_b}{\partial y} \right) \right] dA \tag{10}$$

where the dot-superscript convention indicates differentiation with respect to the time variable t; ρ is the mass density; and I_0 and I_2 are mass inertias defined as

$$\left(I_0,\ I_2\right) = \int_{-h/2}^{h/2} \left(1,\ z^2\right) \rho dz = \left(\rho h,\ \frac{\rho h^3}{12}\right) \tag{11}$$

Substituting the expressions for (δU_P, δU_F, δV, δK) from Eqs. (7) to (10) into Eq. (6), integrating through the thickness of the plate, and collecting the coefficients of δw_b and δw_s, the equations of motion are obtained as

$$\delta w_b: \frac{\partial^2 M_x}{\partial x^2} + 2\frac{\partial^2 M_{xy}}{\partial x \partial y} + \frac{\partial^2 M_y}{\partial y^2} - K_w\left(w_b + w_s\right) + K_s \Delta\left(w_b + w_s\right) + \tilde{N} + q$$
$$= I_0\left(\ddot{w}_b + \ddot{w}_s\right) - I_2 \Delta \ddot{w}_b \tag{12a}$$

$$\delta w_s: \frac{\partial Q_x}{\partial x} + \frac{\partial Q_y}{\partial y} - K_w\left(w_b + w_s\right) + K_s \Delta\left(w_b + w_s\right) + \tilde{N} + q = I_0\left(\ddot{w}_b + \ddot{w}_s\right) \tag{12b}$$

where $\Delta = \partial^2/\partial x^2 + \partial^2/\partial y^2$, and $\tilde{N}$ is defined as

$$\tilde{N} = N_x^0 \frac{\partial^2\left(w_b + w_s\right)}{\partial x^2} + 2N_{xy}^0 \frac{\partial^2\left(w_b + w_s\right)}{\partial x \partial y} + N_y^0 \frac{\partial^2\left(w_b + w_s\right)}{\partial y^2}$$

The boundary conditions are obtained as

- Simply supported (S)

$$w_b = M_n = w_s = 0 \tag{13a}$$

- Clamped (C)

$$w_b = w_{b,n} = w_s = 0 \tag{13b}$$

- Free (F)

$$M_{n,n} + 2M_{ns,s} + \left(K_s + N_n^0\right)\left(w_b + w_s\right)_{,n} + N_{ns}^0\left(w_b + w_s\right)_{,s} + I_2 \ddot{w}_{b,n} = 0$$
$$M_n = Q_n + \left(K_s + N_n^0\right)\left(w_b + w_s\right)_{,n} + N_{ns}^0\left(w_b + w_s\right)_{,s} = 0 \tag{13c}$$

Substituting Eq. (5) into Eq. (1) and using Eq. (2) result in the moments and the transverse shear forces

$$\begin{Bmatrix} M_x \\ M_y \\ M_{xy} \end{Bmatrix} = -D \begin{bmatrix} 1 & \nu & 0 \\ \nu & 1 & 0 \\ 0 & 0 & \frac{1-\nu}{2} \end{bmatrix} \begin{Bmatrix} \frac{\partial^2 w_b}{\partial x^2} \\ \frac{\partial^2 w_b}{\partial y^2} \\ 2\frac{\partial^2 w_b}{\partial x \partial y} \end{Bmatrix} \tag{14a}$$

$$\begin{Bmatrix} Q_x \\ Q_y \end{Bmatrix} = A^s \begin{bmatrix} 1 & 0 \\ 0 & 1 \end{bmatrix} \begin{Bmatrix} \frac{\partial w_s}{\partial x} \\ \frac{\partial w_s}{\partial y} \end{Bmatrix} \tag{14b}$$

where A^s and D are stiffness coefficients of the plate defined as

$$A^s = \frac{\kappa E h}{2\left(1+\nu\right)} \text{ and } D = \frac{E h^3}{12\left(1-\nu^2\right)}$$

with a parameter κ as a shear correction factor.

Substituting Eq. (14) into Eq. (12), the equations of motion can be expressed in terms of displacements w_b and w_s as

$$-D\Delta\Delta w_b - K_w(w_b + w_s) + K_s\Delta(w_b + w_s) + \tilde{N} + q$$
$$= I_0(\ddot{w}_b + \ddot{w}_s) - I_2\Delta\ddot{w}_b \tag{15a}$$

$$A^s \Delta w_s - K_w\left(w_b + w_s\right) + K_s \Delta\left(w_b + w_s\right) + \tilde{N} + q = I_0\left(\ddot{w}_b + \ddot{w}_s\right) \tag{15b}$$

Equation (15) yields the equations of motion of the CPT when the effect of transverse shear deformation is ignored ($w_s = 0$).

3. Analytical Solutions for Rectangular Plates

3.1 Navier Solutions for Simply Supported Plates

Consider a simply supported rectangular plate with length a, width b and thickness h resting on the Pasternak foundations under a transverse load q and in-plane compressive edge forces in two directions ($N_x^0 = \gamma_1 N_0$, $N_y^0 = \gamma_2 N_0$, $N_{xy}^0 = 0$) as shown in Fig. 1. Note that ($\gamma_1 = -1$, $\gamma_2 = -1$) means that the plate is subjected to biaxial compression with the value of N_0. ($\gamma_1 = -1$, $\gamma_2 = 0$) and ($\gamma_1 = 0$, $\gamma_2 = -1$) mean uniaxial compression in the x– and y–axis directions, respectively. Based on the Navier method, the boundary conditions of the simply supported plate are satisfied by the following forms of the variables w_b and w_s:

$$w_b\left(x,\ y,\ t\right) = \sum_{m=1}^{\infty}\sum_{n=1}^{\infty} W_{bmn} e^{i\omega_{mn}t} \sin\alpha x \sin\beta y$$
$$w_s\left(x,\ y,\ t\right) = \sum_{m=1}^{\infty}\sum_{n=1}^{\infty} W_{smn} e^{i\omega_{mn}t} \sin\alpha x \sin\beta y \tag{16}$$

where W_{bmn} and W_{smn} are coefficients; ω is the natural frequency; $i = \sqrt{-1}$; $\alpha = m\pi/a$; $\beta = n\pi/b$. The transverse load q can also be expanded in the double Fourier series form as

$$q\left(x,\ y\right) = \sum_{m=1}^{\infty}\sum_{n=1}^{\infty} Q_{mn} \sin\alpha x \sin\beta y \tag{17}$$

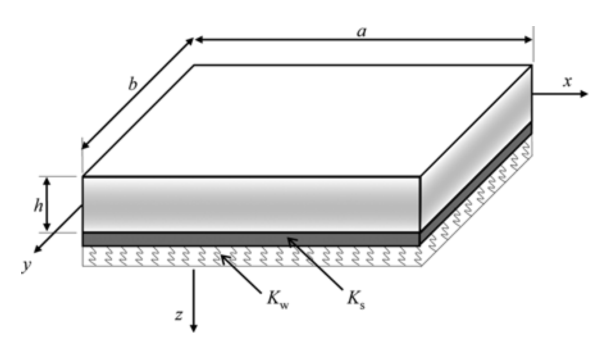

Fig. 1. Geometry and Coordinates of a Simply Supported Plate on Elastic Foundations

where

$$Q_{mn} = \frac{4}{ab}\int_0^a\int_0^b q(x,\ y)\sin\alpha x\sin\beta y\,dx\,dy$$

For a sinusoidal load, the load coefficient Q_{mn} is given by

$$Q_{mn} = \begin{cases} q_0 & (m=1 \text{ and } n=1) \\ 0 & (\text{otherwise}) \end{cases}$$

For a uniform load, the load coefficient Q_{mn} is given by

$$Q_{mn} = \begin{cases} \dfrac{16q_0}{\pi^2 mn} & (m=1,\ 3,\ 5,\ \cdots \text{ and } n=1,\ 3,\ 5,\ \cdots) \\ 0 & (\text{otherwise}) \end{cases}$$

Substituting Eqs. (16) and (17) into Eq. (15), the closed-form solutions can be obtained from

$$\left(\begin{bmatrix} s_{11} & s_{12} \\ s_{12} & s_{22} \end{bmatrix} + p\begin{bmatrix} 1 & 1 \\ 1 & 1 \end{bmatrix} - \omega^2\begin{bmatrix} m_{11} & m_{12} \\ m_{12} & m_{22} \end{bmatrix}\right)\begin{Bmatrix} W_{bmn} \\ W_{smn} \end{Bmatrix} = \begin{Bmatrix} Q_{mn} \\ Q_{mn} \end{Bmatrix} \quad (18)$$

where

$$s_{11} = D\left(\alpha^2+\beta^2\right)^2 + K_w + K_s\left(\alpha^2+\beta^2\right), \quad s_{12} = K_w + K_s\left(\alpha^2+\beta^2\right),$$
$$s_{22} = A^s\left(\alpha^2+\beta^2\right) + K_w + K_s\left(\alpha^2+\beta^2\right), \quad p = N_0\left(\gamma_1\alpha^2+\gamma_2\beta^2\right),$$
$$m_{11} = I_0 + I_2\left(\alpha^2+\beta^2\right), \quad m_{12} = m_{22} = I_0$$

For bending analysis, the closed-form solutions can be obtained by setting the buckling load N_0 and the natural frequency ω in Eq. (18) equal to zero. Thus, the closed-form solutions of the deflections are

$$w_b = \sum_{m=1}^{\infty}\sum_{n=1}^{\infty}\left(\frac{s_{22}-s_{12}}{s_{11}s_{22}-s_{12}^2}\right)Q_{mn}\sin\alpha x\sin\beta y$$

$$w_s = \sum_{m=1}^{\infty}\sum_{n=1}^{\infty}\left(\frac{s_{11}-s_{12}}{s_{11}s_{22}-s_{12}^2}\right)Q_{mn}\sin\alpha x\sin\beta y$$

$$w = w_b + w_s = \sum_{m=1}^{\infty}\sum_{n=1}^{\infty}\left(\frac{s_{11}+s_{22}-2s_{12}}{s_{11}s_{22}-s_{12}^2}\right)Q_{mn}\sin\alpha x\sin\beta y \quad (19)$$

For buckling analysis, the closed-form solution can be obtained by setting the natural frequency ω and transverse load Q_{mn} in Eq. (18) equal to zero. The resulting equation takes the form of an eigenvalue problem, and so the closed-form solution of the buckling load N_0 is

$$N_0(m,\ n) = -\frac{1}{\gamma_1\alpha^2+\gamma_2\beta^2}\frac{s_{11}s_{22}-s_{12}^2}{s_{11}+s_{22}-2s_{12}} \quad (20)$$

Clearly, for each pair of m and n, there is a unique value of N_0 The critical buckling load is the smallest of all $N_0(m, n)$.

$$N_{cr} = \min_{1\le m,n\le\infty}\left[N_0(m,\ n)\right] \quad (21)$$

For free vibration analysis, the closed-form solution is obtained by setting the buckling load N_0 and the transverse load Q_{mn} in Eq. (18) equal to zero. The resulting equation takes the form of an eigenvalue problem. Thus, the closed-form solution of the natural frequency ω can be obtained from the following equation

$$\left(m_{11}m_{22}-m_{12}^2\right)\omega^4 - \left(s_{11}m_{22}+s_{22}m_{11}-2s_{12}m_{12}\right)\omega^2 + \left(s_{11}s_{22}-s_{12}^2\right) = 0 \quad (22)$$

3.2 Lévy Solutions for Other Boundary Conditions

Consider a rectangular plate with two opposite edges simply supported as shown in Fig. 2. Its two opposite edges along $x = 0$, a are simply supported, and the other two edges at $y = \pm b/2$ can each be simply supported, clamped or free. From Eq. (13), the arbitrary boundary conditions at $y = \pm b/2$ can be expressed as follows:

- Simply supported (S)

$$w_b = M_y = w_s = 0 \quad (23a)$$

- Clamped (C)

$$w_b = w_{b,y} = w_s = 0 \quad (23b)$$

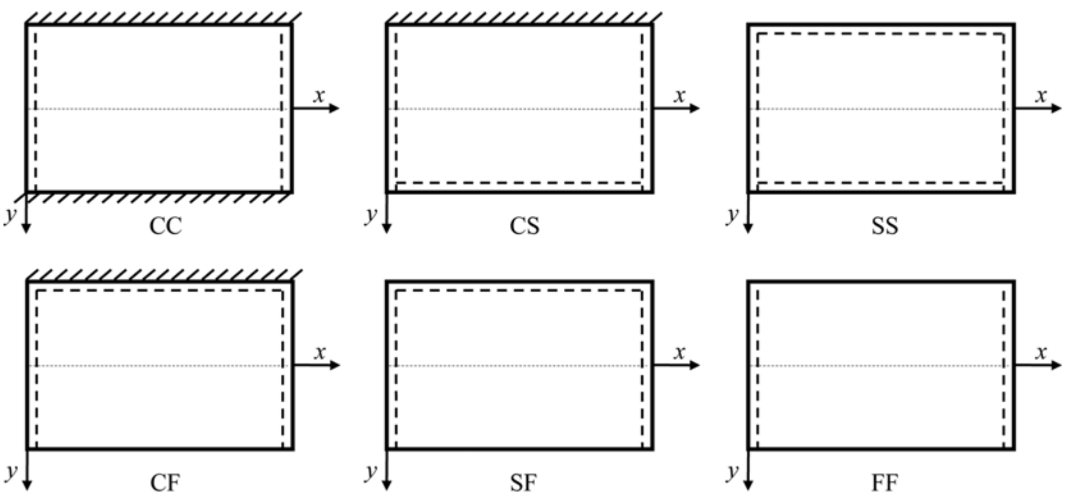

Fig. 2. Boundary Conditions and Coordinates of Lévy-type Plates

- Free (F)

$$2M_{xy,x} + M_{y,y} + N_{xy}^0\left(w_b + w_s\right)_{,x} + \left(K_s + N_y^0\right)\left(w_b + w_s\right)_{,y} + I_2\ddot{w}_{b,y} = 0$$
$$M_y = Q_y + N_{xy}^0\left(w_b + w_s\right)_{,x} + \left(K_s + N_y^0\right)\left(w_b + w_s\right)_{,y} = 0 \tag{23c}$$

Based on the Lévy method, the boundary conditions of the plate are satisfied by the following forms of the variables w_b and w_s:

$$w_b\left(x,\ y,\ t\right) = \sum_{m=1}^{\infty} W_{bm}\left(y\right)e^{i\omega t}\sin\alpha x$$
$$w_s\left(x,\ y,\ t\right) = \sum_{m=1}^{\infty} W_{sm}\left(y\right)e^{i\omega t}\sin\alpha x \tag{24}$$

where W_{bm} and W_{sm} are coefficients; ω is the natural frequency; $i = \sqrt{-1}$; $\alpha = m\pi/a$. The transverse load q can also be expanded in the single Fourier series form as

$$q\left(x,\ y\right) = \sum_{m=1}^{\infty} Q_m\left(y\right)\sin\alpha x \tag{25}$$

where

$$Q_m\left(y\right) = \frac{2}{a}\int_0^a q\left(x,\ y\right)\sin\alpha x\,dx$$

For a sinusoidal load, the load coefficient Q_m is given by

$$Q_m = \begin{cases} q_0 & (m=1) \\ 0 & (\text{otherwise}) \end{cases}$$

For a uniform load, the load coefficient Q_m is given by

$$Q_m = \begin{cases} \dfrac{4q_0}{\pi m} & (m = 1,\ 3,\ 5,\ \cdots) \\ 0 & (\text{otherwise}) \end{cases}$$

Substituting Eqs. (14) and (24) into Eq. (23), the boundary condition at $y = \pm b/2$ can be expressed in terms of the coefficients W_{bm} and W_{sm} as follows:

- Simply supported (S)

$$W_{bm} = \nu\alpha^2 W_{bm} - W''_{bm} = W_{sm} \tag{26a}$$

- Clamped (C)

$$W_{bm} = W'_{bm} = W_{sm} \tag{26b}$$

- Free (F)

$$\left[\left(2-\nu\right)D\alpha^2 + K_s + \gamma_2 N_0 - \omega^2 I_2\right]W'_{bm} - DW'''_{bm} + \left(K_s + \gamma_2 N_0\right)W'_{sm} = 0$$
$$\nu\alpha^2 W_{bm} - W''_{bm} = \left(K_s + \gamma_2 N_0\right)W'_{bm} + \left(A^s + K_s + \gamma_2 N_0\right)W'_{sm} = 0 \tag{26c}$$

where $(\ )' = d(\ )/dy$.

To obtain the analytical solutions by Lévy method, the equation of motion in Eq. (15a) should be changed to different form. Subtracting Eq. (15a) from Eq. (15b), Eqs. (15a) and (15b) can be combined as follows:

$$D\Delta\Delta w_b + A^s\Delta w_s = I_2\Delta\ddot{w}_b$$

or

$$\frac{\partial^2 w_s}{\partial y^2} = -\frac{D}{A^s}\Delta\Delta w_b - \frac{\partial^2 w_s}{\partial x^2} + \frac{I_2}{A^s}\Delta\ddot{w}_b \tag{27}$$

Substituting Eq. (27) into Eq. (15a), Eq. (15) can be rewritten as

$$-\bar{D}\Delta\Delta w_b - K_w\left(w_b + w_s\right) + K_s\Delta w_b + N_x^0\frac{\partial^2\left(w_b + w_s\right)}{\partial x^2} + 2N_{xy}^0\frac{\partial^2\left(w_b + w_s\right)}{\partial x\partial y} + N_y^0\left(\frac{\partial^2 w_b}{\partial y^2} - \frac{\partial^2 w_s}{\partial x^2}\right) + q = I_0\left(\ddot{w}_b + \ddot{w}_s\right) - \bar{I}_2\Delta\ddot{w}_b \tag{28a}$$

$$A^s\Delta w_s - K_w\left(w_b + w_s\right) + K_s\Delta\left(w_b + w_s\right) + \tilde{N} + q = I_0\left(\ddot{w}_b + \ddot{w}_s\right) \tag{28b}$$

where

$$\bar{D} = \left(1 + \frac{K_s + N_y^0}{A^s}\right)D \quad \text{and} \quad \bar{I}_2 = \left(1 + \frac{K_s + N_y^0}{A^s}\right)I_2$$

Substituting Eqs. (24) and (25) into Eq. (28), Eq. (28) can be reduced to ordinary differential equations in y as

$$W_{bm}^{\text{iv}} = C_1 W_{bm} + C_2 W''_{bm} + C_3 W_{sm} + \hat{Q}_{m1}$$
$$W''_{sm} = C_4 W_{bm} + C_5 W''_{bm} + C_6 W_{sm} + \hat{Q}_{m2} \tag{29}$$

where

$$C_1 = -\alpha^4 - \frac{K_w + \left(K_s + \gamma_1 N_0\right)\alpha^2 - \omega^2\left(I_0 + \bar{I}_2\alpha^2\right)}{\bar{D}}, \quad C_2 = 2\alpha^2 + \frac{K_s + \gamma_2 N_0 - \omega^2\bar{I}_2}{\bar{D}},$$
$$C_3 = -\frac{K_w + \left(\gamma_1 - \gamma_2\right)N_0\alpha^2 - \omega^2 I_0}{\bar{D}}, \quad C_4 = \frac{K_w + \left(K_s + \gamma_1 N_0\right)\alpha^2 - \omega^2 I_0}{A^s + K_s + \gamma_2 N_0},$$
$$C_5 = -\frac{K_s + \gamma_2 N_0}{A^s + K_s + \gamma_2 N_0}, \quad C_6 = \frac{A^s\alpha^2 + K_w + \left(K_s + \gamma_1 N_0\right)\alpha^2 - \omega^2 I_0}{A^s + K_s + \gamma_2 N_0},$$
$$\hat{Q}_{m1} = \frac{Q_m}{\bar{D}}, \quad \hat{Q}_{m2} = -\frac{Q_m}{A^s + K_s + \gamma_2 N_0}$$

By the state-space approach, Eq. (29) can be expressed in a system of a first-order matrix differential equation as

$$\left\{Z'\left(y\right)\right\} = \left[T\right]\left\{Z\left(y\right)\right\} + \left\{F\right\} \tag{30}$$

where

$$\left\{Z\right\} = \begin{Bmatrix} W_{bm} \\ W'_{bm} \\ W''_{bm} \\ W'''_{bm} \\ W_{sm} \\ W'_{sm} \end{Bmatrix}, \quad \left[T\right] = \begin{bmatrix} 0 & 1 & 0 & 0 & 0 & 0 \\ 0 & 0 & 1 & 0 & 0 & 0 \\ 0 & 0 & 0 & 1 & 0 & 0 \\ C_1 & 0 & C_2 & 0 & C_3 & 0 \\ 0 & 0 & 0 & 0 & 0 & 1 \\ C_4 & 0 & C_5 & 0 & C_6 & 0 \end{bmatrix}, \quad \left\{F\right\} = \begin{Bmatrix} 0 \\ 0 \\ 0 \\ \hat{Q}_{m1} \\ 0 \\ \hat{Q}_{m2} \end{Bmatrix}$$

The solution to Eq. (30) is given by

$$\mathbf{Z}\left(y\right) = e^{\mathbf{T}y}\left(\mathbf{K} + \int_0^y e^{-\mathbf{T}\xi}\mathbf{F}\left(\xi\right)d\xi\right) = \mathbf{G}\left(y\right)\mathbf{K} + \mathbf{H}\left(y\right) \tag{31}$$

where $e^{\mathbf{T}y}$ denotes the matrix product

$$e^{\mathbf{T}y} = \left[E\right]\begin{bmatrix} e^{\lambda_1 y} & & 0 \\ & \ddots & \\ 0 & & e^{\lambda_6 y} \end{bmatrix}\left[E\right]^{-1}$$

Here [E] is the matrix of distinct eigenvectors of the matrix [T]; $[E]^{-1}$ denotes its inverse; $\lambda_i (i = 1, 2, 3, \ldots, 6)$ are the eigenvalues associated with the matrix [T]; and {K} is a vector of constants to be determined from the boundary conditions at $y = \pm b/2$ [Eq. (26)]. Substituting Eq. (31) into Eq. (26), a nonhomogeneous system of equations is obtained as

$$[M]\{K\} = \{R\} \tag{32}$$

which can be solved for the vector {K}. For buckling and free vibration analyses, $\{R\} = 0$ by setting the transverse load $Q_m = 0$. Thus, the buckling load N_0 and natural frequency ω are determined by setting the determinant of [M] equal to zero.

4. Results and Discussion

In this section, various numerical examples are presented and discussed to verify the accuracy of the present theory. Comparative study is carried out for rectangular plates with a range of values of the aspect ratio a/b, the side-to-thickness ratio a/h and the foundation parameters. The Navier method is used for simply supported plates shown in Fig. 1, and the Lévy method is used for other plates with arbitrary boundary conditions shown in Fig. 2. For these Lévy-type plates, two-letter notations are used to denote the boundary conditions on the edges at $y = \pm b/2$. For instance, SF indicates that the edge at $y = -b/2$ is simply supported (S), and the edge at $y = +b/2$ is free (F). The foundation parameters depend not only on the properties of foundations and structures but also on the load distribution and the depth of the foundation continuum (Turhan, 1992). The values of foundation parameters can be estimated using analytical methods (Girija Vallabhan and Das, 1988; 1991a; 1992b), and existing studies are referred to for verification purposes. In all examples, the value of Poisson's ratio ν is 0.3, and the shear correction factor κ is taken as 5/6. For convenience, the following normalized results are used:

$$\bar{w} = \frac{1000Dw}{q_0 a^4}, \quad \bar{Q}_x = \frac{Q_x}{q_0 a}, \quad \bar{Q}_y = \frac{Q_y}{q_0 a},$$
$$\bar{M}_x = \frac{100M_x}{q_0 a^2}, \quad \bar{M}_y = \frac{100M_y}{q_0 a^2}, \quad \bar{M}_{xy} = \frac{100M_{xy}}{q_0 a^2},$$
$$\bar{N}_0 = \frac{N_0 b^2}{D}, \quad \bar{N}_{cr} = \frac{N_{cr} b^2}{D}, \quad \bar{\omega} = \omega a^2 \sqrt{\frac{\rho h}{D}}, \quad \hat{\omega} = \frac{\omega b^2}{\pi^2} \sqrt{\frac{\rho h}{D}}$$
$$\bar{K}_w = \frac{K_w a^4}{D}, \quad \bar{K}_s = \frac{K_s a^2}{D}, \quad \hat{K}_w = \frac{K_w b^4}{D}, \quad \hat{K}_s = \frac{K_s b^2}{D} \tag{33}$$

4.1 Bending Problem

To verify the accuracy of the present theory, comparative study is carried out for simply supported square plates on elastic foundations under uniform loads. The deflections $\bar{w}$ are presented in Table 1, and the moments $\bar{M}_x$, $\bar{M}_{xy}$ and the transverse shear forces $\bar{Q}_x$ are presented in Table 2 for different values of the side-to-thickness ratio a/h, the foundation parameters $\bar{K}_w$ and $\bar{K}_s$. The results are compared with those by Han and Liew (1997) based on the FSDT, and Thai *et al.* (2013) based on the Refined Plate Theory (RPT). It can be seen that the results of the present theory are in excellent agreement with those of the conventional theories for all values of a/h, $\bar{K}_w$ and $\bar{K}_s$. It should be noted that the present theory involves two variables while the conventional FSDT contains three, so it can be concluded that the present theory is not only accurate but also efficient in predicting the responses of plates.

In Table 3, the deflections $\bar{w}$ of square plates on elastic foundations under uniform loads are presented for various boundary conditions with a range of values of $\bar{K}_w$, $\bar{K}_s$ and a/h. The results are compared with those by Thai *et al.* (2013) based on the RPT. It can be seen that the present theory provides good predictions for

Table 1. Comparison of the Deflections $\bar{w}$ (a/2, b/2) of Simply Supported Square Plates on Elastic Foundations Under Uniform Loads

a/h	$\bar{K}_w$	$\bar{K}_s$	Theory		
			FSDT [a]	RPT [b]	Present
5	1	5	3.7069	3.7061	3.7067
		10	2.9810	2.9806	2.9808
		15	2.4906	2.4904	2.4905
		20	2.1375	2.1373	2.1373
	3^4	5	3.0859	3.0855	3.0857
		10	2.5623	2.5621	2.5622
		15	2.1893	2.1892	2.1892
		20	1.9104	1.9103	1.9102
	5^4	5	1.4029	1.4032	1.4028
		10	1.2809	1.2811	1.2807
		15	1.1784	1.1785	1.1782
		20	1.0911	1.0912	1.0909
10	1	5	3.3455	3.3455	3.3455
		10	2.7505	2.7504	2.7504
		15	2.3331	2.3331	2.3330
		20	2.0244	2.0244	2.0243
	3^4	5	2.8422	2.8421	2.8421
		10	2.3983	2.3983	2.3983
		15	2.0730	2.0730	2.0729
		20	1.8245	1.8244	1.8244
	5^4	5	1.3785	1.3785	1.3784
		10	1.2615	1.2615	1.2614
		15	1.1627	1.1627	1.1627
		20	1.0782	1.0782	1.0782
200	1	5	3.2200	3.2200	3.2200
		10	2.6684	2.6684	2.6684
		15	2.2763	2.2763	2.2763
		20	1.9834	1.9834	1.9834
	3^4	5	2.7552	2.7552	2.7552
		10	2.3390	2.3390	2.3389
		15	2.0306	2.0306	2.0306
		20	1.7932	1.7932	1.7932
	5^4	5	1.3688	1.3688	1.3688
		10	1.2543	1.2543	1.2542
		15	1.1572	1.1572	1.1572
		20	1.0740	1.0740	1.0740

[a]Han and Liew (1997)
[b]Thai *et al.* (2013)

Table 2. Comparison of the Moments $\overline{M}_x$ (a/2, b/2), $\overline{M}_{xy}$ (0, 0) and the Transverse Forces $\overline{Q}_x$ (0, b/2) of Simply Supported Square Plates on Elastic Foundations under Uniform Loads

a/h	$\overline{K}_w$	$\overline{K}_s$	$\overline{M}_x$ (a/2, b/2)		$\overline{M}_{xy}$ (0, 0)		$\overline{Q}_x$ (0, b/2)	
			FSDT[a]	Present	FSDT[a]	Present	FSDT[a]	Present
5	1	5	3.5713	3.5713	-2.5298	-2.5296	0.2700	0.2693
		10	2.8408	2.8408	-2.0846	-2.0844	0.2273	0.2267
		15	2.3517	2.3518	-1.7777	-1.7775	0.1973	0.1967
		20	2.0025	2.0026	-1.5524	-1.5523	0.1750	0.1744
	3^4	5	2.9270	2.9270	-2.1743	-2.1741	0.2379	0.2372
		10	2.4073	2.4073	-1.8440	-1.8439	0.2055	0.2049
		15	2.0404	2.0405	-1.6040	-1.6038	0.1816	0.1810
		20	1.7682	1.7683	-1.4211	-1.4210	0.1631	0.1625
	5^4	5	1.2002	1.2003	-1.1925	-1.1923	0.1485	0.1478
		10	1.0951	1.0951	-1.0938	-1.0936	0.1371	0.1365
		15	1.0069	1.0070	-1.0103	-1.0101	0.1274	0.1268
		20	0.9319	0.9320	-0.9387	-0.9386	0.1190	0.1184
10	1	5	3.6900	3.6901	-2.6183	-2.6182	0.2797	0.2790
		10	2.9915	2.9916	-2.2082	-2.2081	0.2416	0.2410
		15	2.5059	2.5060	-1.9165	-1.9163	0.2142	0.2136
		20	2.1500	2.1501	-1.6975	-1.6974	0.1935	0.1928
	3^4	5	3.0832	3.0833	-2.2859	-2.2858	0.2498	0.2491
		10	2.5678	2.5679	-1.9751	-1.9749	0.2206	0.2199
		15	2.1936	2.1937	-1.7438	-1.7437	0.1987	0.1980
		20	1.9104	1.9105	-1.5645	-1.5643	0.1815	0.1808
	5^4	5	1.3340	1.3341	-1.3086	-1.3084	0.1612	0.1606
		10	1.2125	1.2125	-1.2137	-1.2135	0.1515	0.1509
		15	1.1108	1.1108	-1.1323	-1.1321	0.1431	0.1425
		20	1.0245	1.0246	-1.0618	-1.0616	0.1357	0.1351
200	1	5	3.7313	3.7313	-2.6483	-2.6490	0.2832	0.2824
		10	3.0451	3.0452	-2.2519	-2.2526	0.2469	0.2461
		15	2.5615	2.5616	-1.9669	-1.9676	0.2207	0.2199
		20	2.2035	2.2035	-1.7516	-1.7522	0.2007	0.1999
	3^4	5	3.1389	3.1390	-2.3248	-2.3255	0.2541	0.2533
		10	2.6260	2.6261	-2.0221	-2.0228	0.2262	0.2254
		15	2.2496	2.2496	-1.7952	-1.7958	0.2052	0.2044
		20	1.9624	1.9625	-1.6183	-1.6190	0.1887	0.1879
	5^4	5	1.3854	1.3854	-1.3517	-1.3524	0.1661	0.1653
		10	1.2573	1.2574	-1.2588	-1.2594	0.1571	0.1563
		15	1.1500	1.1500	-1.1789	-1.1796	0.1493	0.1486
		20	1.0589	1.0589	-1.1096	-1.1102	0.1426	0.1418

[a]Han and Liew (1997)

Table 3. Comparison of the Deflections $\overline{w}$ (a/2, 0) of Square Plates on Elastic Foundations with Various Boundary Conditions Under Uniform Loads

$\overline{K}_w$	$\overline{K}_s$	a/h	Theory	Boundary Conditions					
				CC	CS	SS	CF	SF	FF
10	10	5	RPT[a]	1.9541	2.3778	2.9271	3.7013	4.4841	6.3673
			Present	1.9703	2.3861	2.9275	3.7108	4.4844	6.3675
		10	RPT[a]	1.6186	2.0930	2.7059	3.3970	4.2653	6.1550
			Present	1.6209	2.0942	2.7060	3.3983	4.2653	6.1550
		100	RPT[a]	1.4947	1.9895	2.6276	3.2867	4.1883	6.0809
			Present	1.4947	1.9895	2.6276	3.2867	4.1883	6.0809
	100	5	RPT[a]	0.5683	0.6045	0.6450	0.8217	0.8725	1.1432
			Present	0.5740	0.6074	0.6451	0.8251	0.8725	1.1432
		10	RPT[a]	0.5305	0.5820	0.6383	0.7978	0.8670	1.1389
			Present	0.5320	0.5828	0.6383	0.7987	0.8670	1.1390
		100	RPT[a]	0.5105	0.5711	0.6364	0.7858	0.8655	1.1380
			Present	0.5104	0.5711	0.6364	0.7857	0.8655	1.1380
100	10	5	RPT[a]	1.7413	2.0698	2.4788	2.8622	3.3678	4.3276
			Present	1.7541	2.0761	2.4790	2.8688	3.3678	4.3276
		10	RPT[a]	1.4747	1.8563	2.3271	2.6661	3.2446	4.2350
			Present	1.4766	1.8573	2.3272	2.6671	3.2446	4.2350
		100	RPT[a]	1.3731	1.7767	2.2724	2.5930	3.2006	4.2023
			Present	1.3731	1.7767	2.2724	2.5930	3.2006	4.2023
	100	5	RPT[a]	0.5479	0.5815	0.6190	0.7739	0.8198	1.0536
			Present	0.5532	0.5842	0.6190	0.7770	0.8198	1.0536
		10	RPT[a]	0.5131	0.5611	0.6132	0.7527	0.8153	1.0504
			Present	0.5145	0.5618	0.6132	0.7535	0.8153	1.0504
		100	RPT[a]	0.4946	0.5511	0.6117	0.7419	0.8143	1.0498
			Present	0.4946	0.5511	0.6117	0.7419	0.8143	1.0498

[a]Thai *et al.* (2013)

various boundary conditions and all values of $\overline{K}_w$, $\overline{K}_s$ and a/h.

To investigate the effects of increasing the values of $\overline{K}_w$ and $\overline{K}_s$, variations of $\overline{w}$, $\overline{Q}_y$ and $\overline{M}_y$ along the central line ($x = a/2$) and $\overline{M}_{xy}$ along the edge line ($x = 0$) are illustrated in Figs. 3-6, respectively. Both values of $\overline{K}_w$ and $\overline{K}_s$ vary from 2^4 to 4^4. It can be seen that $\overline{K}_s$ has greater influences on the deflection, the transverse shear force and the moments than $\overline{K}_w$. $\overline{K}_w$ also exerts great influences when the value of $\overline{K}_s$ is small, but when the value of $\overline{K}_s$ becomes large, the effect of $\overline{K}_w$ can be ignored.

4.2 Buckling Problem

In Table 4, the critical buckling loads $\overline{N}_{cr}/\pi^2$ of thin square plates ($a/h = 1000$) on elastic foundations under two types of in-plane loads are presented for various boundary conditions with different values of $\hat{K}_w$ and $\hat{K}_s$. The results are compared with those by Lam *et al.* (2000) based on the CPT using Green's functions, Akhavan *et al.* (2009a) based on the FSDT and Thai *et al.* (2013) based on the RPT. It can be seen that the results of the present theory are in excellent agreement with those of the CPT, the FSDT and the RPT for all types of the in-plane loads, various boundary conditions and all values of $\hat{K}_w$ and $\hat{K}_s$.

In Table 5, another comparison of the critical buckling loads $\overline{N}_{cr}$ of rectangular plates ($a/b = 0.5$) on elastic foundations under uniaxial compression ($\gamma_1 = -1, \gamma_2 = 0$) is shown for various boundary conditions with a range of values of $\overline{K}_w$, $\overline{K}_s$ and a/h. The results are compared with those by Akhavan *et al.* (2009a) based on the FSDT and Thai *et al.* (2013) based on the RPT. It can be found that the results of the present theory are in good agreement with those of the conventional theories for various boundary conditions and all values of $\overline{K}_w$, $\overline{K}_s$ and a/h.

Table 6 shows the buckling loads $\overline{N}_0$ of simply supported rectangular plates ($a/b = 2$ and $h/b = 0.15$) on Winkler foundations ($\hat{K}_s = 0$) under biaxial compression with a range of values of $\hat{K}_w$. The results are compared with those by Wang *et al.* (1997) based on the third-order shear deformation theory (TSDT), and it can

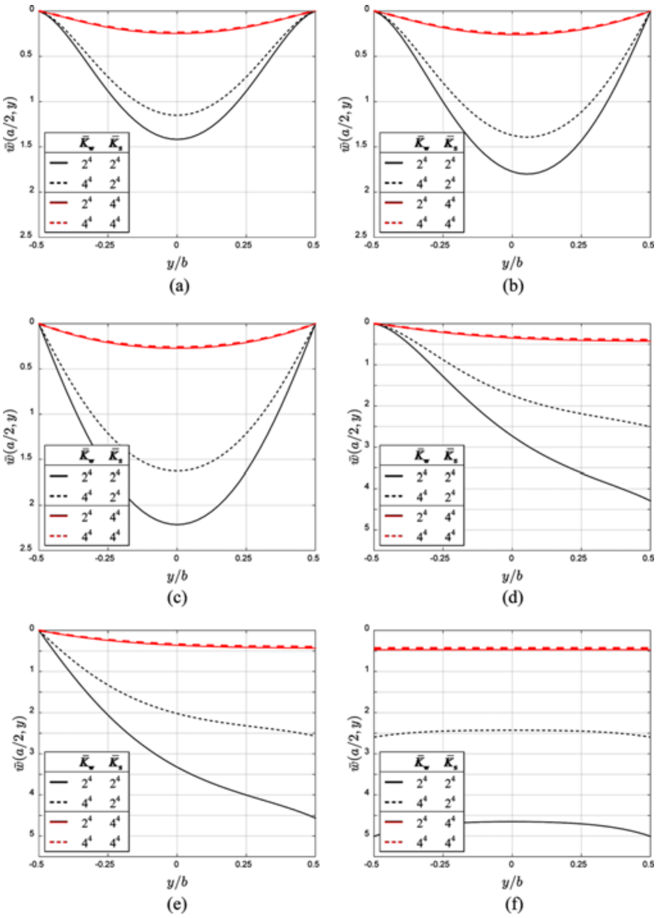

Fig. 3. Variations of the Deflections $\overline{w}$ (a/2, y) for Square Plates (a/h = 10) on Elastic Foundations with Various Boundary Conditions Under Uniform Loads: (a) CC, (b) CS, (c) SS, (d) CF, (e) SF, (f) FF

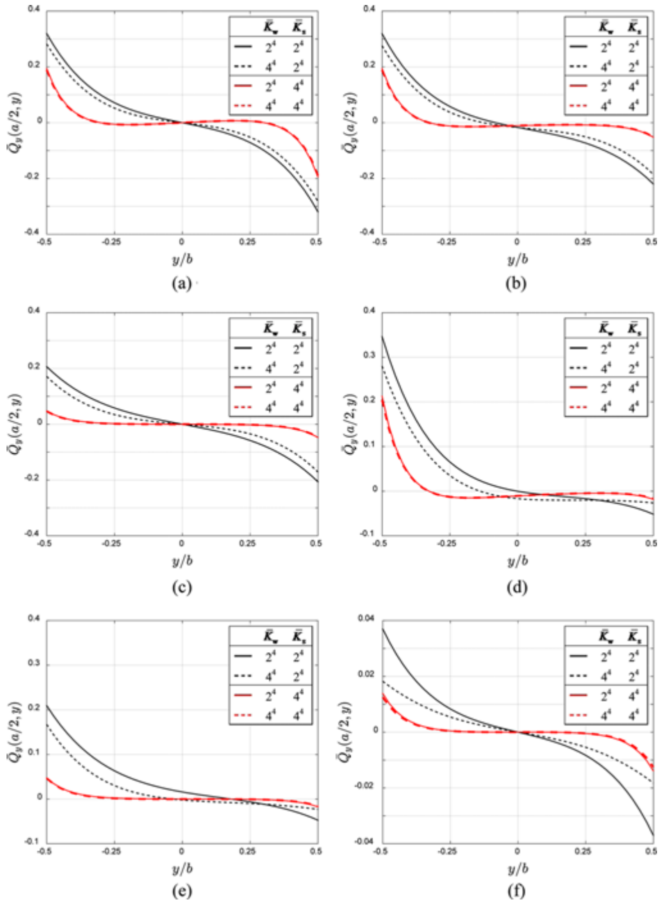

Fig. 4. Variations of the Transverse Shear Forces $\overline{Q}_y$ (a/2, y) for Square Plates (a/h = 10) on Elastic Foundations with Various Boundary Conditions Under Uniform Loads: (a) CC, (b) CS, (c) SS (d) CF, (e) SF, (f) FF

be seen that the results of the present theory are in excellent agreement with those of the TSDT. The boldface values denote the critical buckling loads $\overline{N}_{cr}$. It can be found that the critical buckling load occurs on a higher mode with a larger value as the value of $\hat{K}_w$ increases. It means that the plate under the biaxial compression has a stronger buckling resistance as the value of $\hat{K}_w$ increases. It should be noted that the critical buckling load for $\hat{K}_w = 1000$ and the corresponding mode are different from those by Wang *et al.* (1997) because Wang *et al.* (1997) consider only the modes $(m, 1)$. The critical buckling load for a plate without foundations generally occurs at n = 1, but this result shows that the critical buckling load can occur at $n \geq 2$ when the plate rests on Winkler foundations with the large value of $\hat{K}_w$ and is subjected to biaxial compression. For better understanding, the critical buckling mode shapes for the range of values of $\hat{K}_w$ are illustrated in Fig. 7.

To investigate the effect of increasing the value of $\hat{K}_s$, the same buckling analysis is carried out for the same plate on Pasternak foundations under biaxial compression with $\hat{K}_w$ = 0 and a range of values of $\hat{K}_s$. The buckling loads $\overline{N}_0$ in various modes are shown in Table 7, and the critical buckling loads $\overline{N}_{cr}$ are set in boldface. It can be seen that the critical buckling load still occurs in the same mode (1, 1) while the value of $\hat{K}_s$ increases but it becomes much larger compared to the previous analysis. It means that $\hat{K}_s$ has a greater influence on the buckling resistance of the plate under the biaxial compression compared to $\hat{K}_w$.

Finally, the same buckling analyses are carried out again for the same plate on elastic foundations under uniaxial compression $(\gamma_1 = -1, \gamma_2 = 0)$ with a range of values of $\hat{K}_w$ and $\hat{K}_s$. For a range of values of $\hat{K}_w$, the buckling loads $\overline{N}_0$ and the critical buckling mode shapes are shown in Table 8 and Fig. 8, respectively. It can be found that the buckling phenomenon occurs on a higher mode with a larger critical buckling load as the value of $\hat{K}_w$ increases. For a range of values of $\hat{K}_s$, the buckling loads $\overline{N}_0$ and the critical buckling mode shapes are shown in Table 9 and Fig. 9, respectively. It can also be found that the buckling phenomenon occurs on a higher mode with a larger critical buckling load as the value of $\hat{K}_s$ increases. It means that the plate under uniaxial compression also has a stronger buckling resistance as the value of $\hat{K}_w$ or $\hat{K}_s$ increases. Comparing the results of the two cases, $\hat{K}_s$ has a greater influence on the buckling resistance of the plate

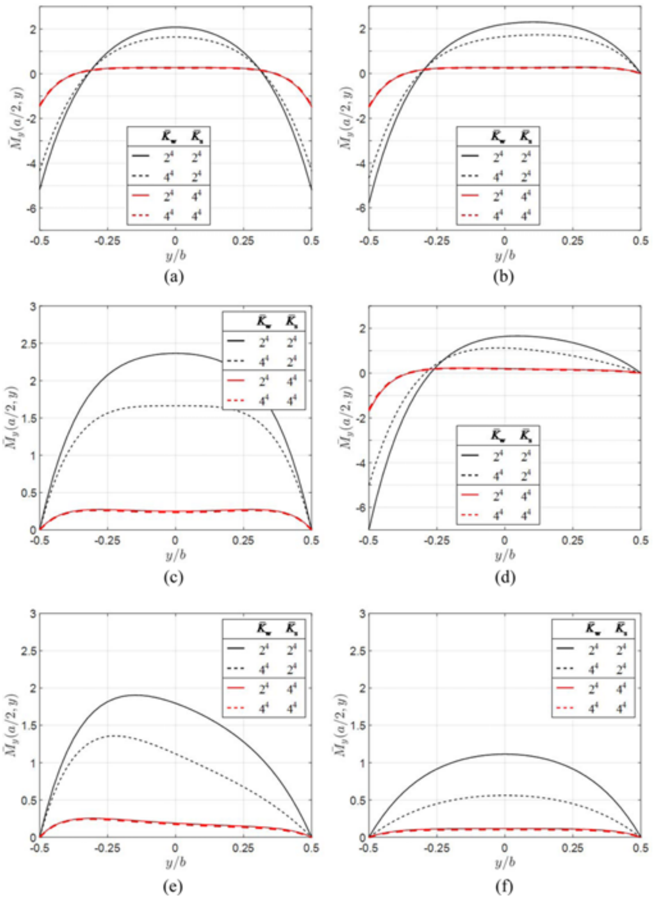

Fig. 5. Variations of the Bending Moments $\overline{M}_y$ (a/2, y) for Square Plates (a/h = 10) on Elastic Foundations with Various Boundary Conditions Under Uniform Loads: (a) CC, (b) CS, (c) SS, (d) CF, (e) SF, (f) FF

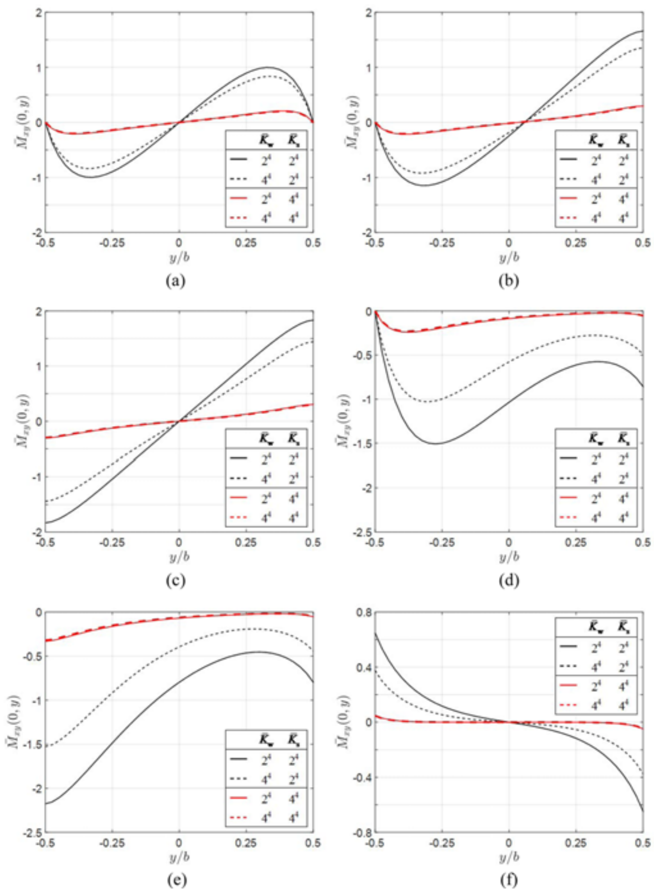

Fig. 6. Variations of the Twisting Moments $\overline{M}_{xy}$ (0, y) for Square Plates (a/h = 10) on Elastic Foundations with Various Boundary Conditions Under Uniform Loads: (a) CC, (b) CS, (c) SS, (d) CF, (e) SF, (f) FF

even under the uniaxial compression.

4.3 Vibration Problem

Table 10 compares fundamental natural frequencies $\overline{\omega}$ of thin square plates $(a/h = 1000)$ on elastic foundations with various boundary conditions and a range of values of $\hat{K}_w$ and $\hat{K}_s$. The results are compared with those by Lam *et al.* (2000) based on the CPT and Thai *et al.* (2013) based on the RPT. It can be observed that the results of the present theory are in excellent agreement with those of the CPT and the RPT for various boundary conditions and all values of $\hat{K}_w$ and $\hat{K}_s$.

Table 11 shows another comparison of the fundamental natural frequencies $\overline{\omega}$ of square plates on elastic foundations with various boundary conditions and a range of values of $\overline{K}_w$, $\overline{K}_s$ and *a*/*h*. The results are compared with those by Akhavan *et al.* (2009b) based on the FSDT and Thai *et al.* (2013) based on the RPT. It has been found that the results of the present theory are in close agreement with those of the conventional theories.

To verify the accuracy of the present theory on higher modes, the first three natural frequencies $\hat{\omega}$ are compared in Table 12 for simply supported square plates on elastic foundations with a range of values of *a*/*h*, $\overline{K}_w$ and $\overline{K}_s$. The results are compared with those by Leissa (1973) based on the CPT; Zhou *et al.* (2004) based on the 3-D elasticity theory using the Ritz method; Dehghan and Baradaran (2011) based on the 3-D elasticity theory using a mixed finite element and differential quadrature method (FE-DQM); Xiang *et al.* (1994) based on the FSDT; and Thai *et al.* (2013) based on the RPT. It can be seen that the results of the present theory are in excellent agreement with those of the conventional theories.

Table 13 shows the first five natural frequencies $\overline{\omega}$ of square plates on elastic foundations to investigate the effects of the values of $\overline{K}_w$ and $\overline{K}_s$ on higher frequencies with different boundary conditions. Increasing the thickness of the plate leads to reducing the natural frequencies regardless of the foundation parameters and the boundary condition. However, increasing the values of the foundation parameters leads to reducing the natural frequencies regardless of the side-to-thickness ratio and the boundary condition. In addition, when the boundary condition changes from FF to CC, the natural frequencies also decrease regardless of the side-to-thickness ratio and the foundation parameters. That is, increasing constraints at the edges of the plate leads to reducing the natural frequencies.

Figure 10 shows the effects of increasing the values of $\overline{K}_w$ or

Table 4. Comparison of the Critical Buckling Loads $\bar{N}_{cr}/\pi^2$ of thin Square Plates (a/h = 1000) on Elastic Foundations with Various Boundary Conditions under In-plane Loads

$\hat{K}_w$	$\hat{K}_s$	Theory	Boundary Conditions					
			CC	CS	SS	CF	SF	FF
Uniaxial Compression ($\gamma_1 = -1$, $\gamma_2 = 0$)								
0	0	CPT[a]	7.691	5.740	4.000	1.653	1.402	0.952
		FSDT[b]	7.69112	5.74015	3.99998	1.65221	1.40141	0.95225
		RPT[c]	7.6912	5.7402	4.0000	1.6525	1.4016	0.9523
		Present	7.6912	5.7402	4.0000	1.6525	1.4016	0.9523
	100	CPT[a]	20.74	19.72	18.92	15.37	15.19	14.07
		FSDT[b]	20.7344	19.7209	18.9151	15.5680	15.6101	14.4168
		RPT[c]	20.7345	19.7210	18.9151	14.8063	14.1697	11.1150
		Present	20.7345	19.7210	18.9151	14.8063	14.1697	11.1150
100	0	CPT[a]	7.948	6.767	5.027	2.679	2.428	1.979
		FSDT[b]	7.94777	6.76675	5.02658	2.67881	2.42801	1.97885
		RPT[c]	7.9478	6.7668	5.0266	2.6791	2.4282	1.9789
		Present	7.9478	6.7668	5.0266	2.6791	2.4282	1.9789
	100	CPT[a]	20.99	19.98	19.17	15.63	15.45	14.33
		FSDT[b]	20.9911	19.9776	19.1717	16.0967	15.8668	14.6734
		RPT[c]	20.9911	19.9776	19.1717	15.6287	15.1963	12.1416
		Present	20.9911	19.9776	19.1717	15.6287	15.1963	12.1416
Biaxial Compression ($\gamma_1 = -1$, $\gamma_2 = -1$)								
0	0	CPT[a]	3.830	2.663	2.000	1.144	1.055	0.932
		RPT[c]	3.8299	2.6627	2.0000	1.1436	1.0551	0.9322
		Present	3.8299	2.6627	2.0000	1.1436	1.0551	0.9322
	100	CPT[a]	13.960	12.800	12.130	11.280	11.190	11.060
		RPT[c]	13.9620	12.7948	12.1321	11.2757	11.1873	11.0643
		Present	13.9620	12.7948	12.1321	11.2757	11.1873	11.0643
100	0	CPT[a]	4.280	3.132	2.513	2.206	1.745	1.626
		RPT[c]	4.2795	3.1320	2.5133	1.7617	1.7452	1.6264
		Present	4.2795	3.1320	2.5133	1.7617	1.7452	1.6264
	100	CPT[a]	14.410	13.260	12.650	11.890	11.880	11.760
		RPT[c]	14.4116	13.2641	12.6454	11.8938	11.8774	11.7585
		Present	14.4116	13.2641	12.6454	11.8938	11.8774	11.7585

[a]Lam *et al.* (2000)
[b]Akhavan *et al.* (2009a)
[c]Thai *et al.* (2013)

Table 5. Comparison of the Critical Buckling Loads $\bar{N}_{cr}$ of Rectangular Plates (a/b = 0.5) on Elastic Foundations with Various Boundary Conditions Under Uniaxial Compression ($\gamma_1 = -1$, $\gamma_2 = 0$)

Boundary Conditions	$(\bar{K}_w, \bar{K}_s)$	a/h	Theory		
			FSDT[a]	RPT[b]	Present
CC	(0, 0)	5	63.4041	64.8257	64.7783
		10	72.2219	72.7916	72.7857
		100	75.8702	75.8774	75.8774
		1000	75.9095	75.9096	75.9096
	(10^2, 10)	5	154.746	156.5788	156.4775
		10	164.081	164.8140	164.7996
		100	168.010	168.0188	168.0187
		1000	168.052	168.0523	168.0523
	(10^3, 10^2)	5	644.041	642.1790	640.8615
		10	691.173	691.6043	691.5106
		100	711.979	711.9900	711.9899
		1000	712.220	712.2204	712.2204
CS	(0, 0)	5	58.2943	58.6678	58.6444
		10	64.9916	65.1441	65.1416
		100	67.6099	67.6118	67.6118
		1000	67.6375	67.6375	67.6375
	(10^2, 10)	5	149.316	149.8982	149.8534
		10	156.268	156.4985	156.4928
		100	159.015	159.0181	159.0181
		1000	159.044	159.0443	159.0443
	(10^3, 10^2)	5	643.768	641.5649	640.3306
		10	688.57	688.4214	688.3658
		100	707.965	707.9651	707.9650
		1000	708.185	708.1850	708.1850
SS	(0, 0)	5	54.3207	54.0737	54.0625
		10	59.6629	59.5856	59.5847
		100	61.6641	61.6633	61.6633
		1000	61.6848	61.6848	61.6848
	(10^2, 10)	5	144.695	144.6022	144.5910
		10	150.191	150.1141	150.1132
		100	152.193	152.1918	152.1918
		1000	152.213	152.2133	152.2133
	(10^3, 10^2)	5	643.500	640.9782	639.8203
		10	686.171	685.5369	685.5126
		100	704.386	704.3775	704.3775
		1000	704.589	704.5888	704.5888

[a]Akhavan *et al.* (2009a)
[b]Thai *et al.* (2013)

Table 6. Comparison of the Buckling Loads $\bar{N}_0$ of Rectangular Plates (a/b = 2, h/b = 0.15) on Winkler Foundations ($\hat{K}_s$ = 0) with a Range of Values of $\hat{K}_w$ under Biaxial Compression ($\gamma_1 = -1$, $\gamma_2 = -1$)

m	n	$\hat{K}_w = 0$		$\hat{K}_w = 100$		$\hat{K}_w = 250$		$\hat{K}_w = 500$		$\hat{K}_w = 1000$	
		TSDT[a]	Present	TSDT[a]	Present	TSDT[a]	Present	TSDT[a]	Present	TSDT[a]	Present
1	1	**11.43**	**11.4305**	**19.54**	**19.5362**	31.69	31.6947	51.96	51.9589	92.49	92.4874
2	1	17.52	17.5165	22.58	22.5825	**30.18**	**30.1816**	42.85	42.8468	68.18	68.1771
3	1	26.59	26.5927	29.71	29.7103	34.39	34.3866	**42.18**	**42.1806**	57.77	57.7684
1	2	-	33.0373	-	35.4213	-	38.9973	-	44.9574	-	**56.8775**
4	1	37.46	37.4633	39.49	39.4897	42.53	42.5293	47.60	47.5954	**57.73**	57.7275
5	1	49.01	49.0102	50.41	50.4078	52.50	52.5041	56.00	55.9979	62.99	62.9856
6	1	60.38	60.3840	61.40	61.3972	62.92	62.9170	65.45	65.4500	70.52	70.5161
7	1	71.05	71.0457	71.81	71.8104	72.96	72.9574	74.87	74.8691	78.69	78.6926
8	1	80.72	80.7191	81.32	81.3151	82.21	82.2091	83.70	83.6991	86.68	86.6792
9	1	89.31	89.3126	89.79	89.7894	90.50	90.5046	91.70	91.6966	94.08	94.0807
10	1	96.85	96.8472	97.24	97.2369	97.82	97.8215	98.80	98.7957	100.74	100.7442

[a]Wang *et al.* (1997)

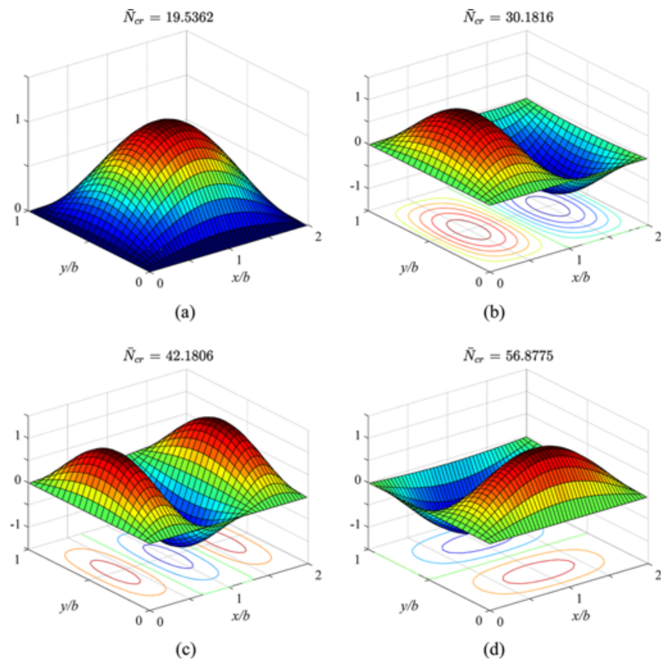

Fig. 7. The Critical Buckling Mode Shapes of Rectangular Plates (a/b = 2, h/b = 0.15) on Winkler Foundations ($\hat{K}_s$ = 0) under Biaxial Compression (γ_1 = –1, γ_2 = –1): (a) $\hat{K}_w$ = 100: (m, n) = (1, 1), (b) $\hat{K}_w$ = 250: (m, n) = (2, 1), (c) $\hat{K}_w$ = 500: (m, n) = (3, 1), (d) $\hat{K}_w$ = 1000: (m, n) = (1, 2)

Table 7. The Buckling Loads $\bar{N}_0$ of Rectangular Plates (a/b = 2, h/b = 0.15) on Pasternak Foundations with $\hat{K}_w$ = 0 and a Range of Values of $\hat{K}_s$ Under Biaxial Compression (γ_1 = –1, γ_2 = –1)

m	n	$\hat{K}_s = 0$	$\hat{K}_s = 100$	$\hat{K}_s = 250$	$\hat{K}_s = 500$	$\hat{K}_s = 1000$
1	1	**11.4305**	**111.430**	**261.430**	**511.430**	**1011.43**
2	1	17.5165	117.516	267.516	517.516	1017.52
3	1	26.5927	126.593	276.593	526.593	1026.59
4	1	37.4633	137.463	287.463	537.463	1037.46
5	1	49.0102	149.010	299.010	549.010	1049.01
6	1	60.3840	160.384	310.384	560.384	1060.38
7	1	71.0457	171.046	321.046	571.046	1071.05
8	1	80.7191	180.719	330.719	580.719	1080.72
9	1	89.3126	189.313	339.313	589.313	1089.31
10	1	96.8472	196.847	346.847	596.847	1096.85

$\bar{K}_s$ to the fundamental natural frequency $\bar{\omega}$. One of these graphs is plotted when $\bar{K}_w$ varies from 10^{-1} to 10^2 with zero $\bar{K}_s$, while the other is plotted when $\bar{K}_s$ varies from 10^{-1} to 10^2 with zero $\bar{K}_w$. It is clearly shown that $\bar{K}_s$ has a higher effect on the natural frequency than $\bar{K}_w$.

5. Conclusions

This paper presents analytical solutions for the bending, buckling and free vibration analyses of isotropic plates resting on elastic foundations using the simplified FSDT. The present theory is more efficient than the conventional FSDT because of its simplicity.

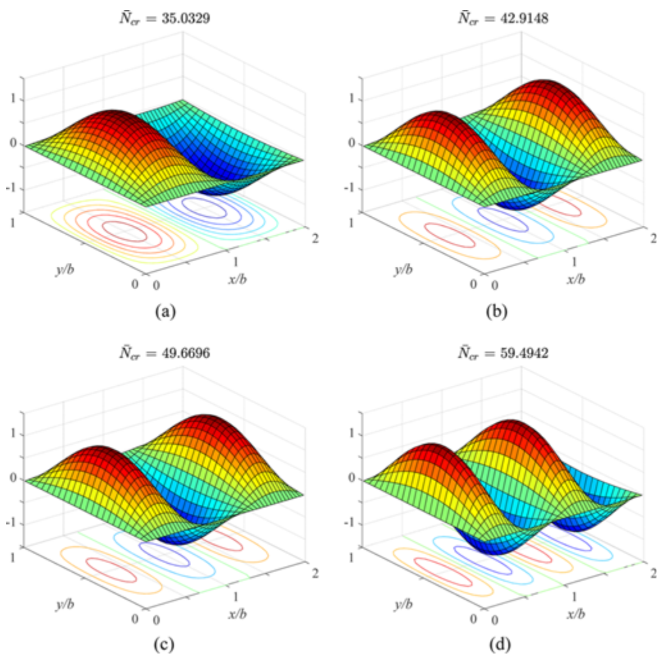

Fig. 8. The Critical Buckling Mode Shapes of Rectangular Plates (a/b = 2, h/b = 0.15) on Winkler Foundations ($\hat{K}_s$ = 0) under Uniaxial Compression (γ_1 = –1, γ_2 = 0): (a) $\hat{K}_w$ = 0: (m, n) = (2, 1), (b) $\hat{K}_w$ = 100: (m, n) = (3, 1), (c) $\hat{K}_w$ = 250: (m, n) = (3, 1), (d) $\hat{K}_w$ = 500: (m, n) = (4, 1)

Table 8. The Buckling Loads $\bar{N}_0$ of Rectangular Plates (a/b = 2, h/b = 0.15) on Winkler Foundations ($\hat{K}_s$ = 0) with a Range of Values of $\hat{K}_w$ under Uniaxial Compression (γ_1 = –1, γ_2 = 0)

m	n	$\hat{K}_w = 0$	$\hat{K}_w = 100$	$\hat{K}_w = 250$	$\hat{K}_w = 500$
1	1	57.1523	97.6808	158.4735	259.7947
2	1	**35.0329**	45.1650	60.3632	85.6935
3	1	38.4117	**42.9148**	**49.6696**	60.9275
4	1	46.8291	49.3621	53.1617	**59.4942**
5	1	56.8519	58.4730	60.9047	64.9576
6	1	67.0933	68.2191	69.9078	72.7222
7	1	76.8453	77.6724	78.9131	80.9809
8	1	85.7640	86.3973	87.3472	88.9303
9	1	93.7231	94.2235	94.9740	96.2249
10	1	100.7211	101.1264	101.7343	102.7475

Table 9. The Buckling Loads $\bar{N}_0$ of Rectangular Plates (a/b = 2, h/b = 0.15) on Pasternak Foundations with $\hat{K}_w$ = 0 and a Range of Values of $\hat{K}_s$ under Uniaxial Compression (γ_1 = –1, γ_2 = 0)

m	n	$\hat{K}_s = 0$	$\hat{K}_s = 100$	$\hat{K}_s = 250$	$\hat{K}_s = 500$
1	1	57.1523	557.152	1307.152	2557.152
2	1	**35.0329**	235.033	535.033	1035.033
3	1	38.4117	182.856	399.523	760.634
4	1	46.8291	**171.829**	359.329	671.829
5	1	56.8519	172.852	346.852	636.852
6	1	67.0933	178.204	**344.871**	622.649
7	1	76.8453	185.009	347.253	617.662
8	1	85.7640	192.014	351.389	**617.014**
9	1	93.7231	198.661	356.069	618.414
10	1	100.7211	204.721	360.721	620.721

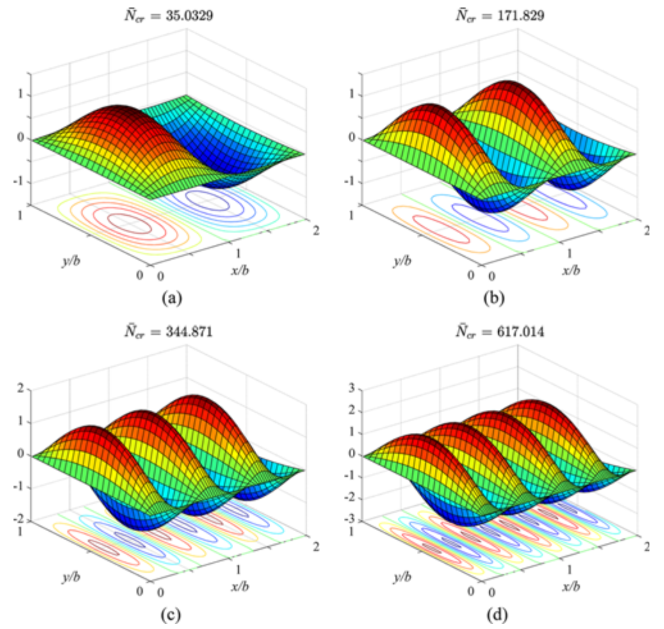

Fig. 9. The Critical Buckling Mode Shapes of Rectangular Plates (a/b = 2, h/b = 0.15) on Pasternak Foundations with $\hat{K}_w$ = 0 under Uniaxial Compression (γ_1 = –1, γ_2 = 0): (a) $\hat{K}_s$ = 0: (m, n) = (2, 1), (b) $\hat{K}_s$ = 100: (m, n) = (4, 1), (c) $\hat{K}_s$ = 250: (m, n) = (6, 1), (d) $\hat{K}_s$ = 500: (m, n) = (8, 1)

Table 11. Comparison of the Fundamental Natural Frequencies $\bar{\omega}$ of Square Plates on Elastic Foundations with Various Boundary Conditions

Boundary Conditions	$(\bar{K}_w, \bar{K}_s)$	a/h	Theory		
			FSDT[a]	RPT[b]	Present
CC	(0, 0)	5	22.5099	23.4965	23.4155
		10	26.7369	27.1825	27.1681
		1000	28.9506	28.9507	28.9507
	$(10^2, 10)$	5	28.2775	29.1749	29.0792
		10	31.9784	32.3934	32.3750
		1000	34.0109	34.0109	34.0109
	$(10^3, 10^2)$	5	58.2962	59.1029	58.9177
		10	61.2251	61.6171	61.5582
		1000	63.1665	63.1665	63.1665
CS	(0, 0)	5	19.7988	20.2138	20.1894
		10	22.4260	22.5954	22.5918
		1000	23.6462	23.6462	23.6462
	$(10^2, 10)$	5	26.1202	26.5058	26.4757
		10	28.3854	28.5454	28.5403
		1000	29.4861	29.4861	29.4861
	$(10^3, 10^2)$	5	57.1091	57.5040	57.4298
		10	59.1455	59.3206	59.2985
		1000	60.2814	60.2814	60.2814

Table 10. Comparison of the Fundamental Natural Frequencies $\bar{\omega}$ of Thin Square Plates (a/h = 1000) on Elastic Foundations with Various Boundary Conditions

$\hat{K}_w$	$\hat{K}_s$	Theory	Boundary Conditions					
			CC	CS	SS	CF	SF	FF
0	0	CPT[a]	28.95	23.65	19.74	12.69	11.68	9.63
		RPT[c]	28.9459	23.6435	19.7374	12.6866	11.6839	9.6310
		Present	28.9507	23.6462	19.7391	12.6873	11.6845	9.6314
	10^2	CPT[b]	54.68	51.32	48.62	37.98	37.15	32.90
		RPT[c]	54.6760	51.3183	48.6149	37.9763	37.1512	32.9039
		Present	54.6810	51.3211	48.6164	37.9772	37.1518	32.9044
	10^3	CPT[b]	146.73	144.24	141.92	112.52	111.71	99.83
		RPT[c]	146.7225	144.2020	141.8731	112.4814	111.7453	99.8311
		Present	146.7415	144.2123	141.8760	112.4851	111.7467	99.8321
10^2	0	CPT[b]	30.63	25.67	22.13	16.15	15.38	13.88
		RPT[c]	30.6245	25.6712	22.1260	16.1539	15.3789	13.8836
		Present	30.6291	25.6738	22.1277	16.1545	15.3795	13.8839
	10^2	CPT[b]	55.59	52.29	49.63	39.27	38.47	34.39
		RPT[c]	55.5829	52.2835	49.6327	39.2708	38.4734	34.3899
		Present	55.5879	52.2863	49.6342	39.2718	38.4741	34.3904
	10^3	CPT[b]	147.13	144.61	142.20	113.00	112.23	100.33
		RPT[c]	147.0628	144.5483	142.2250	112.9250	112.1918	100.3307
		Present	147.0819	144.5586	142.2280	112.9287	112.1933	100.3317
10^3	0	CPT[b]	42.87	39.49	37.28	34.07	33.71	31.62
		RPT[c]	42.8698	39.4838	37.2763	34.0723	33.7118	30.8065
		Present	42.8735	39.4860	37.2778	34.0730	33.7124	33.0570
	10^2	CPT[b]	63.17	60.28	58.00	49.42	48.79	45.64
		RPT[c]	63.1618	60.2787	57.9945	49.4183	48.7871	45.6360
		Present	63.1665	60.2814	57.9961	49.4193	48.7879	45.6366
	10^3	CPT[b]	150.12	147.62	145.43	116.92	116.12	104.72
		RPT[c]	150.0914	147.6285	145.3545	116.8420	116.1335	104.7198
		Present	150.1102	147.6387	145.3575	116.8456	116.1350	104.7208

[a]Leissa (1969), [b]Lam *et al.* (2000), [c]Thai *et al.* (2013)

Table 11. (continued)

Boundary Conditions	$(\bar{K}_w, \bar{K}_s)$	a/h	Theory		
			FSDT[a]	RPT[b]	Present
SS	(0, 0)	5	17.5055	17.4523	17.4486
		10	19.0840	19.0653	19.0650
		1000	19.7391	19.7391	19.7391
	$(10^2, 10)$	5	24.3074	24.2722	24.2699
		10	25.6368	25.6232	25.6229
		1000	26.2112	26.2112	26.2112
	$(10^3, 10^2)$	5	56.0359	56.0309	56.0308
		10	57.3969	57.3921	57.3920
		1000	57.9961	57.9961	57.9961

[a]Akhavan *et al.* (2009b), [b]Thai *et al.* (2013)

Table 12. Comparison of the First Three Natural Frequencies $\hat{\omega}$ of Simply Supported Square Plates on Elastic Foundations

a/h	$\bar{K}_w$	$\bar{K}_s$	Theory	Modes		
				1	2	3
10	200	0	3-D Ritz[b]	2.3951	4.8262	7.2338
			3-D FE-DQM[c]	2.3903	4.8098	7.2186
			FSDT[d]	2.3989	4.8194	7.2093
			RPT[e]	2.3989	4.8198	7.2108
			Present	2.3989	4.8194	7.2093
	1000	0	3-D Ritz[b]	3.7008	5.5661	7.7335
			3-D FE-DQM[c]	3.6978	5.5521	7.7193
			FSDT[d]	3.7212	5.5844	7.7353
			RPT[e]	3.7213	5.5847	7.7366
			Present	3.7212	5.5844	7.7353
	200	10	3-D Ritz[b]	2.7756	5.2954	7.7279
			3-D FE-DQM[c]	2.7721	5.2800	7.7132
			FSDT[d]	2.7842	5.3043	7.7287
			RPT[e]	2.7842	5.3047	7.7300
			Present	2.7842	5.3043	7.7287
	1000	10	3-D Ritz[b]	3.9566	5.9757	8.1954
			3-D FE-DQM[c]	3.9542	5.9623	8.1816
			FSDT[d]	3.9805	6.0078	8.2214
			RPT[e]	3.9805	6.0082	8.2227
			Present	3.9805	6.0078	8.2214
100	100	0	CPT[a]	2.2420	5.1016	8.0639
			3-D Ritz[b]	2.2413	5.0973	8.0527
			3-D FE-DQM[c]	2.2450	5.1643	8.1338
			FSDT[d]	2.2413	5.0971	8.0523
			RPT[e]	2.2413	5.0973	8.0523
			Present	2.2413	5.0971	8.0523
	500	0	CPT[a]	3.0221	5.4894	8.3146
			3-D Ritz[b]	3.0214	5.4850	8.3035
			3-D FE-DQM[c]	3.0242	5.5474	8.3821
			FSDT[d]	3.0215	5.4850	8.3032
			RPT[e]	3.0215	5.4850	8.3032
			Present	3.0215	5.4850	8.3032
	100	10	3-D Ritz[b]	2.6551	5.5717	8.5406
			3-D FE-DQM[c]	2.6578	5.6265	8.6152
			FSDT[d]	2.6551	5.5718	8.5405
			RPT[e]	2.6551	5.5718	8.5405
			Present	2.6551	5.5718	8.5405
	500	10	3-D Ritz[b]	3.3398	5.9285	8.7775
			3-D FE-DQM[c]	3.3420	5.9800	8.8500
			FSDT[d]	3.3400	5.9287	8.7775
			RPT[e]	3.3400	5.9287	8.7775
			Present	3.3400	5.9287	8.7775

[a]Leissa (1973), [b]Zhou *et al.* (2004), [c]Dehghan and Baradaran (2011), [d]Xiang *et al.* (1994), [e]Thai *et al.* (2013)

Table 13. The First Five Natural Frequencies $\bar{\omega}$ of Square Plates on Elastic Foundations with Various Boundary Conditions

Boundary Conditions	$(\bar{K}_w, \bar{K}_s)$	a/h	Modes				
			1	2	3	4	5
CC	(0, 0)	5	23.4155	40.8765	66.4071	95.4122	125.7340
		10	27.1681	49.8012	87.4579	135.0944	188.9646
		1000	28.9507	54.7425	102.2142	170.3411	258.6012
	$(10^2, 10)$	5	29.0792	47.2769	73.6138	103.6672	135.2219
		10	32.3750	55.3926	93.2318	141.1474	195.4087
		1000	34.0109	60.0575	107.4598	175.5111	263.7216
	$(10^3, 10^2)$	5	58.9177	85.1036	119.7306	158.7217	199.9479
		10	61.5582	91.2726	134.3746	186.9105	245.7889
		1000	63.1665	95.2831	146.4109	216.5442	305.9679
CS	(0, 0)	5	20.1894	39.3784	65.7289	95.0717	125.5466
		10	22.5918	47.3729	86.1335	134.3050	188.4614
		1000	23.6462	51.6738	100.2679	168.9533	257.5318
	$(10^2, 10)$	5	26.4757	45.9334	72.9730	103.3371	135.0376
		10	28.5403	53.1675	91.9665	140.3796	194.9148
		1000	29.4861	57.2087	105.5811	174.1502	262.6651
	$(10^3, 10^2)$	5	57.4298	84.1242	119.1664	158.3891	199.7420
		10	59.2985	89.7258	133.3780	186.2581	245.3488
		1000	60.2814	93.1878	144.8618	215.3440	304.9988
SS	(0, 0)	5	17.4486	38.1522	65.1453	94.7658	125.3733
		10	19.0650	45.4827	85.0380	133.6213	188.0114
		1000	19.7391	49.3476	98.6942	167.7781	256.5976
	$(10^2, 10)$	5	24.2699	44.8167	72.4160	103.0388	134.8663
		10	25.6229	51.4180	90.9130	139.7119	194.4720
		1000	26.2112	55.0333	104.0553	172.9951	261.7410
	$(10^3, 10^2)$	5	56.0308	83.2532	118.6573	158.0825	199.5488
		10	57.3920	88.4198	132.5123	185.6758	244.9473
		1000	57.9961	91.4875	143.5621	214.3072	304.1426
CF	(0, 0)	5	11.6537	33.2731	61.2509	91.6347	122.8031
		10	12.3978	38.8931	78.9260	128.1014	183.0725
		1000	12.6873	41.7016	90.6099	159.2976	247.7276
	$(10^2, 10)$	5	18.9625	39.9660	68.4552	99.8204	132.2070
		10	19.6073	45.0053	84.8636	134.2151	189.5375
		1000	19.8698	47.6245	96.0966	164.6028	252.9418
	$(10^3, 10^2)$	5	48.1949	77.1013	113.7137	153.9950	196.0875
		10	49.0453	81.2643	126.1697	179.9974	239.8496
		1000	49.4193	83.6031	135.7122	206.2146	295.7036
SF	(0, 0)	5	10.8310	32.9717	61.1173	91.5672	122.7656
		10	11.4479	38.4638	78.6939	127.9638	182.9857
		1000	11.6845	41.1963	90.2926	159.0756	247.5627
	$(10^2, 10)$	5	18.3278	39.6844	68.3250	99.7535	132.1695
		10	18.8496	44.5971	84.6353	134.0782	189.4508
		1000	19.0583	47.1393	95.7823	164.3810	252.7764
	$(10^3, 10^2)$	5	47.7673	76.8676	113.5886	153.9241	196.0448
		10	48.4981	80.9275	125.9630	179.8667	239.7641
		1000	48.7879	83.1803	135.4143	205.9945	295.5353
FF	(0, 0)	5	9.0306	31.4514	59.9304	90.6268	121.9994
		10	9.4674	36.4817	76.9027	126.3906	181.6129
		1000	9.6314	38.9447	87.9853	156.7480	245.2306
	$(10^2, 10)$	5	16.6046	38.1325	67.0976	98.7756	131.3699
		10	16.9616	42.6096	82.8292	132.4901	188.0641
		1000	17.1011	44.8899	93.4689	162.0475	250.4393
	$(10^3, 10^2)$	5	44.8861	74.7763	111.9932	152.6527	194.9968
		10	45.4288	78.4922	123.9173	178.1119	238.2435
		1000	45.6366	80.5144	132.9204	203.5640	293.1352

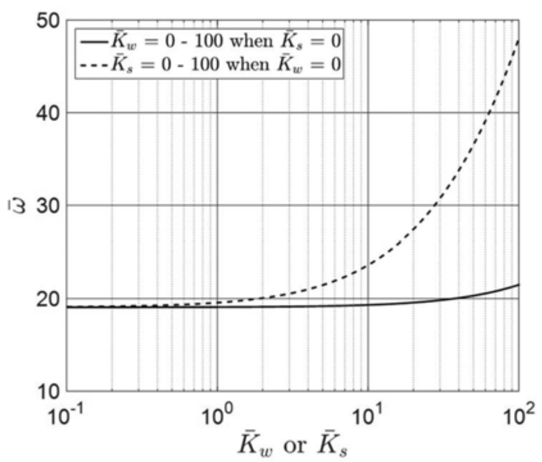

Fig. 10. Variations of the Fundamental Natural Frequencies $\bar{\omega}$ of Square Plates (*a*/*h* = 10) on Elastic Foundations Versus Foundation Stiffness Coefficients $\bar{K}_w$ or $\bar{K}_s$

The accuracy of the present theory has been demonstrated for the bending, buckling and free vibration analyses of rectangular plates resting on elastic foundations with various boundary conditions and a range of values for aspect ratios, side-to-thickness ratios and foundation parameters. It has been found that the deflections, the moments and the transverse shear forces, the buckling loads and the natural frequencies predicted by the present theory (with two variables) are in good agreement with those predicted by the conventional FSDT (with three variables), the HSDTs and 3-D theories. The comparative study shows that the present theory is accurate and efficient in predicting the bending, buckling and free vibration responses of isotropic plates resting on elastic foundations.

Acknowledgements

This research was supported by the Basic Science Research Program through the National Research Foundation of Korea (NRF), funded by the Ministry of Education, Science and Technology (NRF-2015R1D1A1A09060113). The authors wish to express their gratitude for this financial support.

References

Abdalla, J. A. and Ibrahim, A. M. (2006). “Development of a discrete Reissner-Mindlin element on Winkler foundation.” *Finite Elements in Analysis and Design*, Vol. 42, Nos. 8-9, pp. 740-748, DOI: 10.1016/j.finel.2005.11.004.

Akhavan, H., Hashemi, S. H., Taher, H. R. D., Alibeigloo, A., and Vahabi, S. (2009a). “Exact solutions for rectangular Mindlin plates under in-plane loads resting on Pasternak elastic foundation. Part I: Buckling analysis.” *Computer Materials Science*, Vol. 44, No. 3, pp. 968-978, DOI: 10.1016/j.commatsci.2008.07.004.

Akhavan, H., Hashemi, S. H., Taher, H. R. D., Alibeigloo, A., and Vahabi, S. (2009b). “Exact solutions for rectangular Mindlin plates under in-plane loads resting on Pasternak elastic foundation. Part II: Frequency analysis.” *Computer Materials Science*, Vol. 44, No. 3, pp. 951-961, DOI: 10.1016/j.commatsci.2008.07.001.

Buczkowski, R. and Torbacki, W. (2001). “Finite element modelling of thick plates on two parameter elastic foundation.” *International Journal of Numerical and Analytical Methods in Geomechanics*, Vol. 25, No. 14, pp. 1409-1427, DOI: 10.1002/nag.187.

Chucheepsakul, S. and Chinnaboon, B. (2002). “An alternative domain/boundary element technique for analyzing plates on two-parameter elastic foundations.” *Engineering Analysis with Boundary Elements*, Vol. 26, No. 6, pp. 547-555, DOI: 10.1016/S0955-7997(02)00007-3.

Civalek, O. (2007a). “Nonlinear analysis of thin rectangular plates on Winkler–Pasternak elastic foundations by DSC–HDQ methods.” *Applied Mathematical Modelling*, Vol. 31, No. 3, pp. 606-624, DOI: 10.1016/j.apm.2005.11.023.

Civalek, O. (2007b). “Three-dimensional vibration, buckling and bending analyses of thick rectangular plates based on discrete singular convolution method.” *International Journal of Mechanical Sciences*, Vol. 49, No. 6, pp. 752-765, DOI: 10.1016/j.ijmecsci.2006.10.002.

Dehghan, M. and Baradaran, G. H. (2011). “Buckling and free vibration analysis of thick rectangular plates resting on elastic foundation using mixed finite element and differential quadrature method.” *Applied Mathematics and Computation*, Vol. 218, No. 6, pp. 2772-2784, DOI: 10.1016/j.amc.2011.08.020.

Endo, M. (2015). “Study on an alternative deformation concept for the Timoshenko beam and Mindlin plate models.” *International Journal of Engineering Science*, Vol. 87, pp. 32-46, DOI: 10.1016/j.ijengsci.2014.11.001.

Endo, M. and Kimura, N. (2007). “An alternative formulation of the boundary value problem for the Timoshenko Beam and Mindlin plate.” *Journal of Sound and Vibration*, Vol. 301, No. 1, pp. 355-373, DOI: 10.1016/j.jsv.2006.10.005.

Eratll, N. and Akoz, A. Y. (1997). “The mixed finite element formulation for the thick plates on elastic foundations.” *Computer & Structures*, Vol. 65, No. 4, pp. 515-529, DOI: 10.1016/S0045-7949(96)00403-8.

Ferreira, A., Castro, L., and Bertoluzza, S. (2011). “Analysis of plates on Winkler foundation by wavelet collocation.” *Meccanica*, Vol. 46, No. 4, pp. 865-873, DOI: 10.1007/s11012-010-9341-9.

Ferreira, A., Roque, C., Neves, A., Jorge, R., and Soares, C. (2010). “Analysis of plates on Pasternak foundations by radial basis functions.” *Computational Mechanics*, Vol. 46, No. 6, pp. 791-803, DOI: 10.1007/s00466-010-0518-9.

Girija Vallabhan, C. V. and Das, Y. C. (1988). “Parametric study of beams on elastic foundations.” *Journal of Engineering Mechanics*, Vol. 114, No. 12, pp. 2072-2082, DOI: 10.1061/(ASCE)0733-9399(1988)114:12(2072).

Girija Vallabhan, C. V. and Das, Y. C. (1991a). “A refined model for beams on elastic foundations.” *International Journal of Solids and Structures*, Vol. 27, No. 5, pp. 629-637, DOI: 10.1016/0020-7683(91)90217-4.

Girija Vallabhan, C. V. and Das, Y. C. (1991b). “Modified Vlasov model for beams on elastic foundations.” *Journal of Geotechnical Engineering*, Vol. 117, No. 6, pp. 956-966, DOI: 10.1061/(ASCE)0733-9410(1991)117:6(956).

Han, J. B. and Liew, K. M. (1997). “Numerical differential quadrature method for Reissner/Mindlin plates on two-parameter foundations.” *International Journal of Mechanical Sciences*, Vol. 39, No. 9, pp. 977-989, DOI: 10.1016/S0020-7403(97)00001-5.

Henwood, D. J., Whiteman, J. R., and Yettram, A. L. (1982). “Fourier series solution for a rectangular thick plate with free edges on an elastic foundation.” *International Journal for Numerical Methods in Engineering*, Vol. 18, No. 12, pp. 1801-1820, DOI: 10.1002/nme.

1620181205.

Huang, M. H. and Thambiratnam, D. P. (2001). "Analysis of plate resting on elastic supports and elastic foundation by finite strip method." *Computer & Structures*, Vol. 79, Nos. 29-30, pp. 2547-2557, DOI: 10.1016/S0045-7949(01)00134-1.

Kobayashi, H. and Sonoda, K. (1989). "Rectangular Mindlin plates on elastic foundations." *International Journal of Mechanical Sciences*, Vol. 31, No. 9, pp. 679-692, DOI: 10.1016/S0020-7403(89)80003-7.

Lam, K. Y., Wang, C. M., and He, X. Q. (2000). "Canonical exact solutions for Levy-plates on two-parameter foundation using Green's functions." *Engineering Structures*, Vol. 22, No. 4, pp. 364-378, DOI: 10.1016/S0141-0296(98)00116-3.

Leissa, A. W. (1969) *Vibration of plates*, National Aeronautics and Space Administration, USA.

Leissa, A. W. (1973). "The free vibration of rectangular plates." *Journal of Sound and Vibration*, Vol. 31, No. 3, pp. 257-293, DOI: 10.1016/S0022-460X(73)80371-2.

Liew, K. M., Han, J. B., Xiao, Z. M., and Du, H. (1996). "Differential quadrature method for Mindlin plates on Winkler foundations." *International Journal of Mechanical Sciences*, Vol. 38, No. 4, pp. 405-421, DOI: 10.1016/0020-7403(95)00062-3.

Liu, F. L. (2000). "Rectangular thick plates on Winkler foundation: differential quadrature element solution." *International Journal of Solids and Structures*, Vol. 37, No. 12, pp. 1743-1763, DOI: 10.1016/S0020-7683(98)00306-0.

Matsunaga, H. (2000). "Vibration and stability of thick plates on elastic foundations." *Journal of Engineering Mechanics*, Vol. 126, No. 1, pp. 27-34, DOI: 10.1061/(ASCE)0733-9399(2000)126:1(27).

Nobakhti, S. and Aghdam, M. M. (2011). "Static analysis of rectangular thick plates resting on two-parameter elastic boundary strips." *European Journal of Mechanics A/Solids*, Vol. 30, No. 3, pp. 442-448, DOI: 10.1016/j.euromechsol.2010.12.016.

Ozgan, K. and Daloglu, A. T. (2007). "Alternative plate finite elements for the analysis of thick plates on elastic foundations." *Structural Engineering and Mechanics*, Vol. 26, No. 1, pp. 69-86, DOI: 10.12989/sem.2007.26.1.069.

Pasternak, P. L. (1954). *On a new method of analysis of an elastic foundation by means of two foundation constants*, Gosudarstvennoe Izdatelstvo Literaturi po Stroitelstvu i Arkhitekture, Moscow, USSR.

Qin, Q. H. (1995). "Hybrid-Trefftz finite element method for Reissner plates on an elastic foundation." *Computer Methods in Applied Mechanics and Engineering*, Vol. 122, Nos. 3-4, pp. 379-392, DOI: 10.1016/0307-904X(94)90357-3.

Reddy, J. N. (2002) *Energy principles and variational methods in applied mechanics*, John Wiley & Sons, Inc., Hobeken, New Jersey, USA.

Shen, H. S. (1999). "Nonlinear bending of Reissner–Mindlin plates with free edges under transverse and in-plane loads and resting on elastic foundations." *International Journal of Mechanical Sciences*, Vol. 41, No. 7, pp. 845-864, DOI: 10.1016/S0020-7403(98)00060-5.

Shen, H. S. (2000). "Nonlinear bending of simply supported rectangular Reissner–Mindlin plates under transverse and in-plane loads and resting on elastic foundations." *Engineering Structures*, Vol. 22, No. 7, pp. 847-856, DOI: 10.1016/S0141-0296(99)00044-9.

Shen, H. S., Yang, J., and Zhang, L. (2001). "Free and forced vibration of Reissner-Mindlin plates with free edges resting on elastic foundations." *Journal of Sound and Vibration*, Vol. 244, No. 2, pp. 299-320, DOI: 10.1006/jsvi.2000.3501.

Shimpi, R. P., Patel, H. G., and Arya, H. (2007). "New first-order shear deformation plate theories." *Journal of Applied Mechanics*, Vol. 74, No. 3, pp. 523-533, DOI: 10.1115/1.2423036.

Thai, H. T. and Choi, D. H. (2011). "A refined plate theory for functionally graded plates resting on elastic foundation." *Composites Science and Technology*, Vol. 71, No. 16, pp. 1850-1858, DOI: 10.1016/j.compscitech.2011.08.016.

Thai, H. T. and Choi, D. H. (2012). "A refined shear deformation theory for free vibration of functionally graded plates on elastic foundation." *Composites Part B: Engineering*, Vol. 43, No. 5, pp. 2335-2347, DOI: 10.1016/j.compositesb.2011.11.062.

Thai, H. T. and Choi, D. H. (2013). "A simple first-order shear deformation theory for laminated composite plates." *Composite Structures*, Vol. 106, pp. 754-763, DOI: 10.1016/j.compstruct.2013.06.013.

Thai, H. T. and Choi, D. H. (2013). "A simple first-order shear deformation theory for the bending and free vibration analysis of functionally graded plates." *Composite Structures*, Vol. 101, pp. 332-340, DOI: 10.1016/j.compstruct.2013.02.019.

Thai, H. T., Park, M., and Choi, D. H. (2013). "A simple refined theory for bending, buckling, and vibration of thick plates resting on elastic foundation." *International Journal of Mechanical Sciences*, Vol. 73, pp. 40-52, DOI: 10.1016/j.ijmecsci.2013.03.017.

Turhan, A. (1992). *A consistent Vlasov model for analysis of plates on elastic foundations using the finite element method*, PhD Thesis, Texas Tech University, Lubbock, Texas, USA.

Wang, C. M., Kitipornchai, S., and Xiang, Y. (1997). "Relationships between buckling loads of Kirchhoff, Mindlin, and Reddy polygonal plates on Pasternak foundation." *Journal of Engineering Mechanics*, Vol. 123, No. 11, pp. 1134-1137, DOI: 10.1061/(ASCE)0733-9399(1997)123:11(1134).

Winkler, E. (1867). *Die Lehre von der Elasticitaet und Festigkeit*, H. Dominicus, Prag.

Xiang, Y. (2003). "Vibration of rectangular Mindlin plates resting on non-homogenous elastic foundations." *Intetnational Journal of Mechanical Sciences,* Vol. 45, Nos. 6-7, pp. 1229-1244, DOI: 10.1016/S0020-7403(03)00141-3.

Xiang, Y., Wang, C. M., and Kitipornchai, S. (1994). "Exact vibration solution for initially stressed Mindlin plates on Pasternak foundations." *International Journal of Mechanical Sciences*, Vol. 36, No. 4, pp. 311-316, DOI: 10.1016/0020-7403(94)90037-X.

Yen, D. H. Y. and Tang, S. C. (1971). "On the vibration of an elastic plate on an elastic foundation." *Journal of Sound and Vibration*, Vol. 14, No. 1, pp. 81-89, DOI: 10.1016/0022-460X(71)90508-6.

Yettram, A. L., Whiteman, J. R., and Henwood, D.J. (1984). "Effect of thickness on the behaviour of plates on foundations." *Computer & Structures*, Vol. 19, No. 4, pp. 501-509, DOI: 10.1016/0045-7949(84)90096-8.

Yin, S., Hale, J. S., Yu, T., Bui, T. Q., and Bordas, S. P. A. (2014). "Isogeometric locking-free plate element: A simple first order shear deformation theory for functionally graded plates." *Composite Structures*, Vol. 118, pp. 121-138, DOI: 10.1016/j.compstruct.2014.07.028.

Zenkour, A. M. (2009). "The refined sinusoidal theory for FGM plates on elastic foundations." *International Journal of Mechanical Sciences*, Vol. 51, No. 11, pp. 869-880, DOI: 10.1016/j.ijmecsci.2009.09.026.

Zenkour, A. M., Allam, M. N. M., Shaker, M. O., and Radwan, A. F. (2011). "On the simple and mixed first-order theories for plates resting on elastic foundations." *Acta Mechanica*, Vol. 220, Nos. 1-4, pp. 33-46, DOI: 10.1007/s00707-011-0453-7.

Zhou, D., Cheung, Y. K., Lo, S. H., and Au, F. T. K. (2004). "Three-dimensional vibration analysis of rectangular thick plates on Pasternak foundation." *International Journal for Numerical Methods in Engineering*, Vol. 59, No. 10, pp. 1313-1334, DOI: 10.1002/nme.915.